Bis(monoacylglycero)phosphate, a new lipid signature of endosome-derived extracellular vesicles

M. Rabia, V. Leuzy, C. Soulage, A. Durand, B. Fourmaux, E. Errazuriz-Cerda, R. Köffel, A. Draeger, P. Colosetti, A. Jalabert, et al.

▶ **To cite this version:**

M. Rabia, V. Leuzy, C. Soulage, A. Durand, B. Fourmaux, et al.. Bis(monoacylglycero)phosphate, a new lipid signature of endosome-derived extracellular vesicles. Biochimie, 2020, 10.1016/j.biochi.2020.07.005 . hal-02902561

HAL Id: hal-02902561
https://hal.science/hal-02902561

Submitted on 24 Oct 2022

HAL is a multi-disciplinary open access archive for the deposit and dissemination of scientific research documents, whether they are published or not. The documents may come from teaching and research institutions in France or abroad, or from public or private research centers.

L'archive ouverte pluridisciplinaire **HAL**, est destinée au dépôt et à la diffusion de documents scientifiques de niveau recherche, publiés ou non, émanant des établissements d'enseignement et de recherche français ou étrangers, des laboratoires publics ou privés.

Distributed under a Creative Commons Attribution - NonCommercial 4.0 International License

Version of Record: https://www.sciencedirect.com/science/article/pii/S0300908420301590
Manuscript_69065b10a291f0eaf369469d71bfe27a

Bis(monoacylglycero)phosphate, a new lipid signature of endosome-derived extracellular vesicles

Maxence Rabia[1], Valentin Leuzy[1], Christophe Soulage[1], Annie Durand[1], Baptiste Fourmaux[1,2], Elisabeth Errazuriz-Cerda[3], René Köffel[4], Annette Draeger[4], Pascal Colosetti[1], Audrey Jalabert[1], Mathilde Di Filippo[1,5], Audrey Villard-Garon[6], Cyrille Bergerot[7], Céline Luquain-Costaz[1], Philippe Moulin[1,6], Sophie Rome[1], Isabelle Delton[1] and Françoise Hullin-Matsuda[1,*]

[1] Univ-Lyon, CarMeN laboratory, Inserm U1060, INRAe U1397, INSA Lyon, Villeurbanne, France

[2] Functional Lipidomics platform, CarMeN laboratory / IMBL-INSA Lyon, 69621 Villeurbanne Cedex, France.

[3] Univ-Lyon, CIQLE (Centre d'Imagerie Quantitative Lyon Est) Rockefeller, Lyon, France

[4] Department of Cell Biology, Institute of Anatomy, University of Bern, Bern, Switzerland

[5] Department of Biochemistry and Molecular Biology, Centre de Biologie et de Pathologie Est, Hospices Civils de Lyon, Bron, France

[6] Department of Endocrinology, Hôpital Cardiovasculaire Louis Pradel, Hospices Civils de Lyon, Lyon, Bron, France

[7] Department of Cardiology, Hôpital Cardiovasculaire Louis Pradel, Hospices Civils de Lyon, Lyon, Bron, France

*to whom correspondence should be addressed: Inserm UMR 1060, CarMeN laboratory, IMBL building, 69621 Villeurbanne cedex, France; Phone: +33 (0)4 72 43 76 27; email : francoise.hullin-matsuda@inserm.fr

Running title: BMP and endosomal-derived extracellular vesicles

© 2020 published by Elsevier. This manuscript is made available under the CC BY NC user license
https://creativecommons.org/licenses/by-nc/4.0/

Abbreviations: BMP, bis(monoacylglycero)phosphate; diC22:6-BMP, di-docosahexaenoyl BMP; CAD, cationic amphiphilic drug; ESCRT, endosomal sorting complexes required for transport; ILV, intraluminal vesicle; LBPA, lysobisphosphatidic acid; LSD, lysosomal storage disorder/disease; NAFLD, nonalcoholic fatty liver disease; NASH, nonalcoholic steatohepatitis; MVE, multivesicular endosome

Abstract

Bis(monoacylglycero)phosphate (BMP), also known as lysobisphosphatidic acid (LBPA), is a phospholipid specifically enriched in the late endosome-lysosome compartment playing a crucial role for the fate of endocytosed components. Due to its presence in extracellular fluids during diseases associated with endolysosomal dysfunction, it is considered as a possible biomarker of disorders such as genetic lysosomal storage diseases and cationic amphiphilic drug-induced phospholipidosis. However, there is no true validation of this biomarker in human studies, nor a clear identification of the carrier of this endolysosome-specific lipid in biofluids. The present study demonstrates that in absence of any sign of renal failure, BMP, especially all docosahexaenoyl containing species, are significantly increased in the urine of patients treated with the antiarrhythmic drug amiodarone. Such urinary BMP increase could reflect a generalized drug-induced perturbation of the endolysosome compartment as observed *in vitro* with amiodarone-treated human macrophages. Noteworthy, BMP was associated with extracellular vesicles (EVs) isolated from human urines and extracellular medium of human embryonic kidney HEK293 cells and co-localizing with classical EV protein markers CD63 and ALIX. In the context of drug-induced endolysosomal dysfunction, increased BMP-rich EV release could be useful to remove excess of undigested material. This first human pilot study not only reveals BMP as a urinary biomarker of amiodarone-induced endolysosomal dysfunction, but also highlights its utility to prove the endosomal origin of EVs, also named as exosomes. This peculiar lipid already known as a canonical late endosome-lysosome marker, may be thus considered as a new lipid marker of urinary exosomes.

Keywords: bis(monoacylglycero)phosphate, docosahexaenoic acid, exosomes, extracellular vesicles, lysobisphosphatidic acid, lysosomal storage diseases

1. Introduction

Bis(monoacylglycero)phosphate (BMP) is an intriguing polyglycerophospholipid due to its exclusive subcellular organelle localization, its unusual lipid structure and the still unresolved enzymatic steps of its *de novo* biosynthesis pathway [1-7]. It is also known as lysobisphosphatidic acid (LBPA), a misleading terminology for its structure of two monoacylglycerols linked through one phosphate group [2, 3]. BMP is found in most mammalian cells and tissues [2]. It is specifically enriched in the late endosome/lysosome, also referred to as endolysosome, where it participates actively in the trafficking of lipids and proteins passing through this acidic compartment. BMP appears progressively during the maturation of the endosome visualized by a multivesicular appearance due to inward budding of the organelle limiting membrane towards its lumen leading to the formation of intraluminal vesicles (ILVs). Whereas it represents only 1% of the total phospholipids in most mammalian tissues, BMP amounts to 15% of the phospholipids of the late endosome and constituting up to 70% of their internal membrane phospholipids, including ILVs [8]. BMP is a structural isomer of phosphatidylglycerol (PG) and displays an unusual *sn*-1-glycerophospho-*sn*-1'-glycerol configuration [9]. This unique stereoconfiguration renders BMP more stable in the acidic organelle environment and resistant to phospholipase potentially explaining its extended lifetime [10]. Several studies from our laboratory and others have demonstrated the role of BMP in the dynamics of the endolysosome membrane including its hijacking during pathogen infection, in cholesterol transport and in sphingolipid degradation [1, 2, 4, 11-14]. Interestingly, BMP and other anionic phospholipids are necessary for RNA virus infection and replication as well as bacterial toxin release as highlighted by the inhibitory effect of anti-BMP antibodies or drug-induced modification of the acidic endosomal pH [4, 15, 16].

Noteworthy, the negative charge of BMP and its unsaturated fatty acid enrichment actively drive ILV formation in endosomes [4, 7, 17, 18]. ILVs are important for the fate of the endocytosed proteins and lipids not only by mediating their transport to the lysosome for degradation, but also by being released as extracellular vesicles (EVs) after fusion of the multivesicular endosomes (MVEs) with the plasma membrane. The name EV refers to a heterogeneous group of membrane vesicles of variable sizes either originated from the endosome compartment often referred to as "exosomes" (about 50 to 120nm in diameter) or from shedding of the plasma membrane often referred to as "microvesicles" (about 50nm to 1μm and even bigger in diameter) [19]. The precise role of BMP to control exosome biogenesis and secretion is still unclear [4, 20]. In addition, contradictory results were published about the presence of BMP in EVs with its absence [21], its low content [22] and its enrichment in case of endolysosomal dysfunction [23]. Such discrepancy could be linked to the lack of sensitivity of the detection method used as well as the variability of exosome secretion according to

the cell type. EVs are found in various biological fluids and involved in different pathophysiological processes linked to the release of their protein, lipid and nucleic acid content that can be used for intercellular communication [19, 24-26].

BMP increase in cells and tissues was reported in various disorders such as cationic amphiphilic drugs (CAD)-induced phospholipidosis and genetic lysosomal storage diseases (LSDs) associated with endolysosomal dysfunction characterized by accumulation of undigested material and secondary metabolites [27-31]. The CAD toxicity, a major concern in drug development, is linked to this build-up of drug and undigested compounds inside the acidic endolysosomal compartment visualized by the formation of vacuoles and concentric multi-lamellar inclusions [32, 33]. BMP and particularly the docosahexaenoic acid (C22:6n-3) containing species such as diC22:6-BMP, was detected also in extracellular fluids (plasma, urines..) during these disorders and thus, considered as a possible biomarker to follow disease progression [34, 35]. However, most of these studies were performed with animal models [36, 37] and are still requiring validation in humans as well as identification of the BMP carrier in extracellular fluids. We hypothesized that BMP in biological fluids could be associated with EVs and a valuable biomarker of CAD-induced endolysosomal dysfunction in humans. With this aim, we performed a first pilot human study with urines of patients treated with amiodarone (Cordarone®), the most frequently used antiarrhythmic drug and a reference compound among the CADs. Amiodarone has a long elimination half-life, highly variable among patients (35 to 110 days). It may require months to reach steady state blood levels (about 0.7 to 3.7 μM). However, plasma levels do not correlate well with efficacity or adverse effects. The onset of action occurs within several hours after intravenous administration (primarily given for emergency treatment of serious arrhythmias) and requires 2 to 3 days after oral administration to outpatients. Because it is a lipophilic drug, it accumulates extensively in the liver, lung, fat, skin and other tissues (thyroid) [38-40]. Significant side effects due to tissue accumulation are observed even with low doses of amiodarone (200 to 300 mg/day) during long-term oral therapy and are not seen with short-term intravenous therapy (800 to 1600 mg/day). It was estimated that the prevalence of side effects can be as high as 15% in the first year and as high as 50% with long-term therapy that can go up to several years. Appropriate follow-up for liver injury or dysthyroidism (usually every 6 months) is essential during long-term treatment to evaluate the risk-benefit ratio. Fortunately, most of amiodarone's side effects are reversible with dose reduction or discontinuation of therapy. Thus, the build-up of phospholipidosis seems a gradual event and the extent and time course of drug trapping inside the late endosome/lysosome compartment appears to vary among patients.

2. Materials and Methods

2.1. Materials

Unless otherwise indicated, most reagents are from VWR Chemicals. Solvents used for lipid analysis are HPLC grade or RPE. Ammonium formate, amiodarone hydrochloride (A842) are from Sigma Aldrich (Saint-Quentin Fallavier, France). Lipid standards are from Avanti Polar Lipids (Alabaster, Alabama, USA). The mouse monoclonal antibodies, anti–CD63 (Cluster of Differentiation CD63 or lamp3; sc-5275), anti-CD81 (CD81 or TAPA-1; sc-166028), anti-ALIX (apoptosis linked gene 2 ALG2-interacting protein X; sc-53540), anti-TSG101 (tumor susceptibility gene 101; sc-7964) are from Santa Cruz Biotechnology (Heidelgerg, Germany). Mouse monoclonal antibody anti-BMP (clone 6C4) is a gift from Dr T. Kobayashi (Univ Strasbourg, France and RIKEN, Japan). Cell culture reagents are from Gibco (ThermoFisher Scientific, Illkirch, France). Macrophage colony-stimulating factor (M-CSF) was purchased from BioLegend (London, UK) and phorbol ester PMA from Sigma.

2.2. Human subject study

Twenty-four ambulatory outpatients receiving oral treatment of amiodarone (=amiodarone group; average oral dose: 200mg/day) were recruited from the outpatient clinic of Endocrinology and Cardiology of "Hospices Civils de Lyon" (HCL). Among them, six amiodarone-treated patients displayed amiodarone-induced dysthyroidism. As it is known that amiodarone can induce liver steatosis [41], we recruited six outpatients from Endocrinology not treated with amiodarone but suffering from nonalcoholic steatohepatitis (=NASH group) to evaluate the specific effect of hepatic dysfunction on urinary BMP concentration for comparison. Twelve healthy volunteers (=Control group) were recruited that matched in age with amiodarone and NASH patients (see **Table 1** for detailed characteristics of subjects). The study was conducted in agreement with the bioethics law Jarde based on the Biobank INSERM UMR 1060 CARMEN_ministerial agreement N°DC-2010-117 and in accordance to the declaration of Helsinki principles. Written informed consent was obtained from all control subjects and patients.

Second morning urines were collected and frozen immediately at -80ºC until analysis. The total urine volume was measured and then, an aliquot was centrifuged 10 min at room temperature (800 x g, Jouan Centrifuge CR 4-12, swinging rotor 11175338). The supernatant devoid of cells and mineral sediments was processed for lipid extraction. In preliminary experiments, we showed that there was no significant difference in the BMP content from whole urines and urine supernatants, indicating that most of urinary BMP is recovered in the soluble and not cellular fraction.

2.3. Animal study

Three month-old male Wistar rats were purchased from Janvier SA (Le Genest- Saint-Isle, France) and housed in an air-conditioned room with a controlled environment of 21 ± 0.5°C and 60-70 % humidity, under a 12h light/dark cycle with free access to food and water. All experimental procedures were performed in accordance with the guidelines laid down by the French Ministry of Agriculture

(n°2013-118) and the European Union Council Directive for the protection of animals used for scientific purposes of September 22nd, 2010 (2010/63UE). All animal experiments were performed under the authorization DDPP-DSV n°69-266-0501 (INSA-Lyon, November 2017). They were divided into 3 groups of 3 rats each. Amiodarone (**supplemental Figure S1A**) was suspended in an aqueous solution of 5% (w/v) glucose, 0.1% (v/v) Tween 80 and administered daily for 8 days by oral gavage of a single dose of 50 mg/kg/day (A50 group, n=3) and 150 mg/kg/day (A150 group, n=3) as previously used [27, 42]. The control group (n=3) only received the aqueous solution of 5% (w/v) glucose solution with 0.1% (v/v) Tween 80. After the last gavage, rats were kept for 24h in metabolic cages (Charles River, L'Abresle, France) with no food but free access to water. The 24h-urines were collected in sodium azide-containing vials and the total volume recorded. At the end of the study, rats were deeply anesthetized with sodium pentobarbital (180mg/kg ip), blood was drawn by direct intracardiac puncture and collected on ethylenediamine tetraacetic acid (EDTA) tubes. Plasma was collected after centrifugation at room temperature (1600 x g, 10 min), aliquoted and stored at -80°C until analysis. Aliquots of the 24h-urines were centrifuged 10 min at room temperature (800 x g, Jouan Centrifuge CR 4-12, swinging rotor 11175338) then urine supernatants were stored at -80°C until analysis. Livers were weighted, washed in ice-cold phosphate buffered saline (PBS) and cut in small pieces. Liver pieces were snap frozen in liquid nitrogen, then crushed and stored at -80° C until analysis. The clearance of creatinine and BMP expressed in ml/min was calculated according to the formula: ([Urine concentration µmol/ml or pmol/ml] x Urine flow) / [Plasma concentration µmol/ml or pmol/ml] with urine flow (ml/min) evaluated after collection of the 24h-urines.

2.4. Cell culture

HEK293 human embryonic kidney cells (ATCC CRL-1573) were grown in Dulbecco's modified Eagle's medium (DMEM) supplemented with 10% fetal bovine serum (FBS), 100U/ml penicillin and 100µg/ml streptomycin in a 5% CO_2-humidified incubator at 37°C. THP-1 human monocytic cells (ATCC TIB-202) were cultured in RPMI 1640 supplemented with 10% FBS, 100U/ml penicillin and 100µg/ml streptomycin in a 5% CO_2-humidified incubator at 37°C. They were differentiated into macrophages by exposure to 50ng/ml phorbol 12-myristate 13-acetate (PMA) for 72h [43, 44].

Human buffy coats from healthy volunteers were purchased with the ethics committee approval of the Red Cross Switzerland (project P_103 to René Köffel). Primary human monocytes from buffy coats were isolated as previously described [45] and differentiated to macrophages in RPMI supplemented with 10% FBS and 1% penicillin–streptomycin with M-CSF (75 ng/ml) for 7 days.

2.5. Lipid extraction and mass spectrometry analysis

Lipid extraction was performed according to the Bligh and Dyer method [46] in acidic conditions as previously described [6, 8]. Briefly samples (urines 1.6ml; urinary EVs 10µl; plasma 1ml; liver powder 500mg) containing 2mM EDTA were extracted by a mixture of chloroform/methanol (1:2 v:v)

containing butylated hydroxytoluene (BHT, 25µM final) and internal standard diC14:0-BMP (urines, 120pmol; plasma, 240 pmol; liver, 600pmol; EVs, 30pmol). The samples were partitioned by addition of chloroform and a solution of 25mM HCl, 154mM NaCl. The lower chloroformic phase was collected, then dried under nitrogen flux. This phospholipid extract was reconstituted by methanol for analysis.

The identification of the molecular species of BMP such as the diC22:6-BMP (**supplemental Figure S1B**) by mass spectrometry was done according to references [9] and [28] with modifications. The analysis was performed by reverse-phase liquid chromatography-tandem mass spectrometry (RPHPLC-MS/MS) using hybrid triple quadrupole linear ion trap mass spectrometer SCiex 4500 QTRAP LC MS/MS equipped with an HPLC system Shimadzu LC-30AD Nexera and a SIL-30AC. Samples (10µl) were injected on an Acquity UPLC^{R} BEH C18 column (Waters) equipped with a Vanguard^{TM} precolumn Acquity UPLC^{R} BEH C18. The temperature of the column was maintained at 60°C. Gradient chromatography to separate BMP from PG was performed with a mixture of solvent B (methanol:acetonitrile: formic acid 70:30:0.1, v/v/v, containing 5 mM ammonium formate) and aqueous solvent A (water: formic acid 100:0.1, v/v , containing 5 mM ammonium formate) at a flow rate of 500 µl/min with acquisition during 45 min. Data were acquired in multiple reaction monitoring (MRM) with positive mode electrospray ionization (ESI). The parameters used for mass spectrometry of BMP are: DP depolarization potential: 101V; CE collision energy: 41 V; Output potential of the CXP collision cell: 10 V; Source temperature: 350 ° C. Ammonium adducts of di C14:0-BMP and di C14:0-PG have similar precursor ion $[M+NH_4]^+$ at mass to charge ratio m/z 684.3 and produced respectively, a monoacylglycerol MAG fragment (m/z 285.3) and a diacylglycerol DAG fragment (m/z 495.6) (**Supplemental Figure S1C**). In the extracted ion LC chromatograms, the triple peaks observed for BMP are regioisomers with different acylation positions on the glycerol moieties (successively: *sn*-2,2'; *sn*-2,3' or *sn*-3,2'; *sn*-3,3') whereas PG shows a single peak that exhibits a longer retention time than BMP [9, 28]. Integration of ion peak area was carried out by Analyst 1.6 software. Lipid concentration was calculated by relating the peak area of each species to the area of the internal standard. Our HPLC-MS/MS analysis allowed us to identify and quantify 20 different molecular species of BMP. The limit of detection per molecular species was about 0.3 or 1.0 pmol/ml for urines and plasma, respectively. BMP content in urines was adjusted to creatinine concentration for sample comparison. Furthermore, the absence of gender difference for urinary BMP secretion allowed us to pool the data from men and women inside each group. Absence of gender-specificity of diC22:6-BMP levels in plasma and urine of healthy subjects has already been reported [37].

2.6. Isolation of extracellular vesicles

Isolation of EVs from urines was done as described by Gheinani *et al*. [47]**.** Urine was processed by successive centrifugations as detailed in the summary chart (**Supplemental Figure S2A**, plain lines). The final EV pellet (P5) was recovered in PBS and stored at -80°C until Western blot, lipid analysis

and transmission electron microscopy analysis. In a second set of experiments (**Supplemental Figure S2A**, dotted lines), the 10 000 × g-pellet (P3) was resuspended in 200 mg/ml dithiothreitol (DTT) 10 min at 37°C to denature the urinary uromodulin or Tamm-Horsfall protein that can lower the final EV yield [48]. The resuspended pellet was processed by successive centrifugations as described (**Supplemental Figure S2A**, dotted lines). The final EV pellet (P5_DTT) was stored at -80°C until Western blot and lipid analysis.

Isolation of EVs from conditioned medium of human HEK293 cells was performed as described in Forterre *et al*. [49]. HEK293 cells were plated in 150 cm^2 flask (10^6 cells), grown to about 70% confluence in complete medium (DMEM + 10% FBS). Then, cells were incubated for 48h in DMEM + 10% EV-depleted FBS. EV-depleted medium was prepared by ultracentrifugation of DMEM + 20% FBS at 100,000 × g for 18 h at 4°C. The resulting EV-depleted supernatant was filtered at 0.2 µm and diluted to 10% with sterile DMEM. HEK293-conditioned medium was centrifuged for EV isolation at 4°C as described above for urinary EV isolation (**Supplemental Figure S2A,** plain lines**).** The EV pellet recovered in PBS was stored at -80°C until analysis.

2.7. Immunofluorescence

Primary human monocytes or human THP-1 cells were plated on glass coverslips in RPMI 1640 supplemented with 10% FBS and differentiated into macrophages as indicated above. They were not treated (=control cells) or treated with 10 µM amiodarone for 24h. At the end of the treatment, Lyso Tracker DND99 Red (Invitrogen Molecular Probes, ThermoFisher Scientific, Illkirch, France) (67nM) was added in the medium for 30 min to label the acidic organelles. Then, cells were fixed with 4% (w/v) paraformaldehyde for 15 min at room temperature and blocked in 1% (w/v) bovine serum albumin BSA-PBS for 30 min. They were incubated with primary antibody: anti-BMP (6C4) 1/10 in 0.1% (w/v) saponin, 1% (w/v) BSA-PBS for 2h, then with secondary antibody labeled with Alexa488 (Jackson ImmunoResearch Labs, ThermoFisher Scientific, Illkirch, France) in 1% (w/v) BSA-PBS for 1h at room temperature. They were mounted in Prolong Gold antifade medium (Invitrogen Molecular Probes P36935) and analyzed with a Zeiss LSM 880 confocal scanning microscope (objective Plan-Apochromat 63x/1.4 oil DICM27).

2.8. Transmission electron microscopy (TEM)

Purified EVs from human urines or from conditioned medium of human HEK293 cells were imaged by TEM after immunogold staining as previously described [49, 50]. Briefly, purified EVs (5µl) were absorbed on 200 mesh nickel grids coated with formvar-C for 2 min at RT. Immunogold labeling performed by flotation of grids on drops of reaction media. Non-specific labeling was blocked with 1% (w/v) BSA and 1% (v/v) normal goat serum in 50mM Tris-HCl, pH 7.4 for 10min at RT. Primary antibody incubation was performed for 1h at RT in a wet chamber with mouse monoclonal antibodies against BMP or CD63 diluted 1/10 or 1/50, respectively in 1% BSA, 50mM Tris-HCl, pH 7.4. Grids

were successively washed at RT with 50mM Tris-HCl, pH 7.4, and then pH 8.2. Then, they were incubated in a wet chamber in 1% BSA, 50 mM Tris-HCl, pH 8.2 for 10 min at RT and labeled for 45min in a wet chamber with goat anti-mouse IgG gold-conjugated (10 nm) (Tebu-Bio, Le Perray-en-Yvelines, France) diluted 1/50 in 1% (w/v) BSA, 50mM Tris-HCl, pH 8.2. Grids were successively washed at RT with 50mM Tris-HCl pH 8.2, and pH 7.4.

For immune-double labeling after blocking nonspecific labeling as above, grids with EV suspensions were first incubated with primary antibody against EV protein marker CD63 (diluted 1/50), then with secondary goat anti-mouse IgG antibody labeled with 5nm gold particles (1/50) as described above. After blocking nonspecific labeling as above, grids were incubated with mouse primary antibody against BMP (diluted 1/10), then with 15 nm gold-conjugated goat anti-mouse IgG antibody (1/50).

The immunocomplex was fixed with 2% (w/v) glutaraldehyde for 2min. Then grids with EV suspensions were colored with 2% (w/v) phosphotungstic acid for 2 min and observed with TEM (Jeol 1400 JEM, Tokyo, Japan) equipped with a Gatan camera (Orius 600) and Digital Micrograph Software. Gold particle was assigned to a vesicle when lying within a distance of 20 to 40 nm from its limiting membrane.

2.9. Western Blot analysis

Western Blot analysis was performed as previously described [14, 49]. Proteins were electrophoresed on 11% SDS-PAGE gels and transferred on PVDF membranes. Unspecific binding was blocked with 5% (w/v) fat-free powdered milk in Tris-buffered saline containing 0.03% (v/v) Tween 20 (TBST). Then, primary antibody was incubated overnight at 4ºC in blocking buffer (4% (w/v) BSA in TBST). Mouse monoclonal antibodies against ALIX, CD81, CD63 and TSG101 were used at 1:5000, 1:2000, 1:500 and 1:2000 dilution, respectively. They were detected with peroxidase-conjugated anti-mouse IgG (Jackson ImmunoResearch Labs), revealed with ECL system (Immobilon Forte, MerckMillipore, Molsheim, France) and observed with an Image Master VDS-CL bio-imaging system (GE Healthcare Life Sciences_Amersham Biosciences, Little Chalfont, England).

2.10. Biological and biochemical analyses

Creatinine was quantified in urine supernatants and plasma using the Multigent Creatinine kit (Enzymatic_ B8L242, Abbott) on Architect® Analyzer (Abbott, Wiesbaden, Germany). Plasma alanine aminotransferase (ALT) and aspartate aminotransferase (AST) were analyzed by routine methods on Architect® Analyzer (Wiesbaden, Germany). Two different assays were used for protein quantification with bovine serum albumin as standard: Bradford Reagent (ref B6916) from Sigma-Aldrich (MERCK/Germany) for urine samples and urinary EVs; and Pierce™ BCA Protein assay kit (ref 23225) from Thermo Fisher Scientific (Massachusetts, USA) for cell samples.

2.11. Statistical analysis

Unpaired two-tailed Student's *t* test was used to determine significant differences between patients versus controls. Significant change was set at $p < 0.05$.

3. Results

3.1 Increase of diC22:6-BMP in the urine of amiodarone-treated rats without any change in renal function

We first explored the link between urinary BMP and the renal function using rats treated with amiodarone as previously reported [51] and quantified selectively the diC22:6-BMP species in liver, urine and plasma. After 8 day-treatment with amiodarone, diC22:6-BMP a major BMP molecular species of rat liver [52] was barely increased in the liver of both amiodarone-treated groups compared to the control group (**Figure 1A**). However, amiodarone treatment induced a dose-dependent increase of the hepatic transaminases AST and ALT in the plasma as well as of the liver weight compared to the control group (**Figure 1A)** suggesting that oral administration of amiodarone induced a toxic dose-dependent hepatitis. DiC22:6-BMP content displayed a two-fold and seventeen-fold increase, respectively in the urine of rats treated with 50 and 150 mg/kg of amiodarone compared to the control group (**Figure 1B)**. In addition, plasma diC22:6-BMP levels showed a two to three-fold increase in both amiodarone-treated groups compared to the control group (**Figure 1C)** suggesting a systemic effect of amiodarone associated with phospholipidosis as previously reported [51].

We then evaluated the renal function after amiodarone treatment. The urinary creatinine concentration as well as the proteinuria were not significantly changed in both amiodarone-treated groups compared to the control group (**Figure 1C)**. In addition, the creatinine clearance was not modified by amiodarone treatment (**Figure 1C),** indicating that the renal function was maintained. Interestingly whereas the diC22:6-BMP clearance was barely detectable in the control group and the lower dose of amiodarone group, its clearance increased in the higher dose of amiodarone group reaching levels close to the creatinine clearance (**Figure 1C**). These results suggest that high dose or accumulation of amiodarone is favoring the secretion of diC22:6-BMP into urine without apparent modification of the renal function.

3.2 Specific increase of all the docosahexaenoyl BMP species in the urine of amiodarone-treated patients

We then analyzed the BMP molecular species variations in urine of human patients treated with amiodarone. All the selected subjects had urinary creatinine concentrations in the normal range without statistically significant difference to the control subjects (**Table 1, Supplemental Figure S3A**) indicating a normal renal function. A significant four fold-increase of the diC22:6-BMP species as well as the total BMP content was found in urine of amiodarone-treated patients compared to the control subjects (**Figure 2A**). Interestingly, detailed analysis of the BMP molecular species showed

that all the docosahexaenoyl species of BMP increased significantly in the urine of amiodarone-treated patients compared to the controls (**Table 2**). The docosahexaenoyl species represented about 33% of the BMP molecular species of the controls and increased to 42% in the amiodarone-treated patients. Besides this enrichment in unsaturated species, diC16:0-BMP species was also present. Significant amounts of diC16:0-BMP were previously reported in human plasma [28]. Interestingly, diC16:0-BMP species represented approximately 41% of the BMP molecular species of the control subjects and decreased to 22% in the amiodarone-treated patients. The schematic representation of the overall amiodarone-induced increase of BMP polyunsaturation is displayed in the **Figure 2B**.

This observation led us to seek for a possible link with a tissue origin of the amiodarone-induced dysfunction focusing on the well-reported side effects of the drug on thyroid [40] as well as on liver [41]. We first compared the urinary BMP content of patients displaying or not an amiodarone-induced dysthyroidism (see **Table 1**, n=6 and n=18, respectively). DiC22:6-BMP species as well as total BMP content were significantly increased in amiodarone-treated patients regardless of their dysthyroidism compared to control subjects (**Supplemental Figure S3B**). These results suggest that the urinary increase of BMP was not selective for the amiodarone-induced thyroid dysfunction. To evaluate the role of hepatic dysfunction, we quantified BMP content in urine of NASH patients not treated with amiodarone (see **Table 1**, n=6). Both diC22:6-BMP and the total BMP amounts displayed only a mild insignificant increase in urine of NASH patients compared to control subjects whereas they were significantly different between amiodarone-treated patients and NASH patients (**Figure 2A**). Furthermore, detailed analysis of the BMP molecular species showed a significant increase of BMP monounsaturated species in NASH patients compared to control subjects whereas change in the BMP docosahexaenoyl species was insignificant (**Table 2** and **Figure 2A**). These results indicate that modification of hepatic function linked to a liver metabolic disorder does not significantly increase diC22:6-BMP as well as total BMP content in the urine. All these results suggest that amiodarone treatment specifically increases diC22:6-BMP as well as all the docosahexaenoyl species of BMP in human urine, results in good agreement with previously reported results in rat including those from our present rat study (**Figure 1**).

3.3 Urinary extracellular vesicles contained the late endosome lipid marker BMP

In order to characterize the carrier of BMP in urine, we purified urinary EVs and analyzed their BMP content. In preliminary experiments, we successfully isolated EVs from urine after successive centrifugations coupled with 0.2µm filtration and use of the reducing agent DTT (see **Supplemental Figure S2A** for purification procedure). The last ultracentrifugation pellet (P5) contains vesicles characterized by Western blot analysis with antibodies against classical EV protein markers CD63, CD81 and ALIX (**Supplemental Figure S2B)** and by Zetasizer Nano analysis displaying an expected size around 77 nm (data not shown). We also confirmed that DTT treatment used to increase the EV yield did not modify BMP detection by LC-MS/MS analysis (data not shown).

We then purified EVs from the urine (50 ml) of 3 control subjects and 3 amiodarone-treated patients previously analyzed for their BMP content (**Figure 2** and **Table 2**). Interestingly, amiodarone treatment induced a significant 2-fold increase of total EV proteins released into the urine compared to control subjects (**Figure 3A**). Western blot analysis using antibodies against CD63, ALIX and TSG101 detected these classical EV markers in the urinary EVs in both types of samples and confirmed the increased release of EVs after amiodarone treatment (**Figure 3B**). Noteworthy, LC-MS/MS analysis of the EV lipid extracts showed that diC22:6-BMP was present in EVs with a 6-fold increase in amiodarone-treated patients compared to control subjects. Similar fold increase of diC22:6-BMP was observed in the 200 x g-urine supernatants (**Figure 3A**). Despite the small number of samples and the quite large variations between them for statistically significant difference, we observed a diDHA-BMP enrichment of EVs in amiodarone-treated patients that displays an average of 2.7 pmol/µg proteins compared to 0.35 pmol/µg proteins in EVs of control subjects.

To confirm the presence of BMP in urinary EVs, we performed immuno-electron microscopy analysis. **Figure 4** shows that urinary EVs were nanovesicles at the expected size between 50 to 120 nm and contained the EV protein marker CD63 **(Fig 4A)** as well as the late endosome lipid marker BMP **(Fig 4B**). Furthermore, these vesicles were co-labeled by BMP and CD63 (**Fig 4C**). Then, we used human embryonic kidney 293 cells (HEK293) known to release EVs in cultured medium as a model of renal cells [24, 53]. Interestingly, immuno-electron microscopy analysis performed on vesicles purified from the conditioned medium of HEK293 cells showed nanovesicles at the expected size for EVs and labeled with the EV protein marker CD63 and BMP **(Figure 5)**. Furthermore, co-labeling for BMP and CD63 was seen in the same vesicles as observed previously with EVs from human urine. Similar results were observed with EVs isolated from the conditioned medium of HEK293 treated for 24hr with 10µM Amiodarone (data not shown). Therefore, our results confirm that a substantial amount of BMP is associated with EVs isolated from human urine as well as culture medium of human embryonic kidney cells. Our co-labelling results as well as the concomitant increase of Alix and CD63 with BMP suggest an endosomal origin of these EVs.

3.4 Amiodarone modifies the endolysosomal compartment of human macrophages

To investigate a possible link between the amiodarone effect on EV secretion and the endosomal compartment, we studied the drug effect in human macrophages. This type of cells are known to be enriched in BMP [7], to secrete EVs [54] and to be sensitive to cationic drugs such as amiodarone [15, 36]. Primary human monocytes and cultured human monocytic THP-1 cells were differentiated into macrophages and treated with 10 µM amiodarone for 24h. In **Figure 6A,** fluorescent confocal microscopy analysis showed that primary human macrophages treated with amiodarone (lower panels) displayed an enlargement of BMP-positive and LysoTracker-positive structures, as compared to control cells (upper panels). A similar size increase of BMP-positive and LysoTracker-positive

organelles was observed after incubation of human THP-1 macrophages with amiodarone (**Figure 6B,** lower panels). Interestingly, amiodarone induced not only the enlargement of the acidic organelles but also a change in their intracellular distribution from a more juxtanuclear to a peripheral distribution. These results suggest that amiodarone interferes with the acidic endosomal compartment and might thus impact EV formation.

4. Discussion

Here we demonstrated that the endolysosomal phospholipid BMP is increased in the urine of amiodarone-treated patients and is associated with endosome-derived EVs characterized as exosomes. To our knowledge, this is the first human study that evaluated the occurence of BMP in the urine of amiodarone-treated patients and analyzed its different molecular species. Our LC-MS/MS method allowed us to identify 20 different molecular species of BMP. Interestingly, all the docosahexaenoyl-containing species and particularly the diC22:6-BMP were increased in the urine of amiodarone-treated patients as observed also in urine and plasma of amiodarone-treated rats. This di-polyunsaturated species exhibits two advantages for quick and reliable detection, due to its early elution time on C18 column before the bulk of the other lipid species and its specific MAG fragment species. This is an important criterion for considering diC22:6-BMP as a convenient biomarker of drug-induced endolysosomal storage disorder.

4.1 BMP, an urinary biomarker of amiodarone-induced endolysosomal dysfunction in humans without renal dysfunction

Amiodarone is one of the reference compound among the CADs inducing phospholipidosis characterized by drug and lipid accumulation in the endolysosome leading progressively to liver, kidney or lung failure [41, 51, 55]. Previous studies in rodents identified BMP and especially the diC22:6 BMP species as a potential biomarker of phospholipidosis induced by various CADs such as amiodarone, chloroquine or azithromycin [27, 36, 37, 51]. In rat, urinary diC22:6-BMP was considered as a better predictor of CAD-induced phospholipidosis compared to other phospholipid species that are increased in urine in case of nephrotoxicity [33]. On the other side, serum levels of diC22:6-BMP in rats displayed a higher correlation with a generalized phospholipidosis, especially in case of amiodarone-induced liver necrosis [27]. In mice, amiodarone treatment increased the total BMP content in liver without significant change of diC22:6-BMP, whereas this species as well as total BMP were increased in plasma [56]. In agreement with those studies, we also found that diC22:6-BMP increased in both plasma and urine, but not in liver of amiodarone-treated rats. Nonalcoholic fatty liver is considered as a risk factor for drug-induced hepatotoxicity [57]. However, our results with NASH patients suggest that modification of hepatic function linked to metabolic syndrome did not significantly increase diC22:6-BMP nor total BMP content in the human urine. This is consistent with recent results reporting unchanged BMP concentration in the serum of NASH patients [56].

Overall, urinary diC22:6-BMP appears useful to monitor the onset and the progression of amiodarone-induced phospholipidosis in rats before any nephrotoxicity or liver necrosis. From our present human pilot study, this may be extrapolated to humans as the increase of diC22:6-BMP in the urine of amiodarone-treated patients was observed in absence of renal dysfunction while this increase was not detected in the urine of NASH patients with hepatic dysfunction and without amiodarone treatment.

Since we did not have access to the blood of the amiodarone-treated patients, we can only speculate on the possible link between the amiodarone-induced increase of BMP in the circulation and in the urine. Presence of BMP in high density lipoproteins (HDLs) was recently demonstrated in mice plasma [56]. In human plasma, BMP was detected partly (40% of plasma BMP in control subjects) or primarily (80% in certain LSDs such as Gaucher disease) associated with lipoproteins (HDLs and very low density lipoproteins VLDLs) [28]. This suggests that BMP found in the circulation may be released by macrophages and liver cells. As a lipophilic cationic drug, amiodarone is sequestered after multiple cycles of macroautophagy in the acidic organelles, especially in macrophages possessing numerous endolysosomes [32, 58, 59]. Our *in vitro* observations that amiodarone modifies the endolysosomal compartment of human primary macrophages suggest that the BMP increase in urine of amiodarone-treated patients could reflect the drug-induced perturbation of this compartment involved in EV biogenesis. Whatever the BMP carrier in the blood (lipoproteins, albumin or perhaps EVs), we know that filterability of molecules through the glomerular capillary wall is mainly based on their size and their electrical charges [60]. We can thus assume that in basal conditions, circulating BMP should not be filtered through the glomerular filtration barrier thus explaining the lower BMP renal clearance compared to that of creatinine, observed in our control rats. After amiodarone treatment and before any kidney damage, BMP increase in the circulation would favor its renal secretion explaining the increased BMP renal clearance noticed in our rat study.

4.2 Amiodarone-induced increase of BMP-containing EVs in human urine

Our human study shows for the first time that amiodarone treatment increased the urinary release of EVs identified by the canonical EV protein markers CD63, ALIX and TSG101 [61, 62]. Noteworthy, part of BMP was associated with EVs in the urine. Urinary EVs have recently gained increasing interest using them as disease biomarkers, mainly in the context of kidney diseases [47, 63-66]. They seemed released by all the epithelial cells lining the urinary tract [64, 67]. Although presence of diC22:6-BMP in urines was already reported in rodents [27, 36, 37, 51], the carrier of BMP has never been identified. EVs are reported in various biological fluids but they represent a heterogeneous group of membrane vesicles of variable sizes (nano to micrometer of diameter) and origins (from endosome or plasma membrane origin) [19]. However, this nomenclature was recently questioned since their biogenesis may differ according to cell type and common intracellular mechanisms and sorting machineries are shared for the formation of the different EV subpopulations [68]. Classically, the term “exosomes” refers to extracellular ILVs released after MVE fusion with the plasma membrane.

Whereas intensive research was performed to identify the various EV protein markers, less work was done on their specific lipid analysis [69, 70]. Based on the specific endolysosomal localization of BMP and its absence in plasma membrane, we can speculate that BMP could be used as a new exosome lipid marker discriminating their endosomal origin. This will require further analysis in EVs isolated from various extracellular biofluids. The role of BMP in EV biogenesis and secretion was already suggested mainly due to its interaction with the endosomal sorting complexes required for transport (ESCRT)-associated protein ALIX [4, 71] and its specific localization in ILVs [8, 72]. Furthermore, the amiodarone-induced enrichment of urinary BMP with docosahexaenoyl species suggests that such polyunsaturation could participate in the BMP secretion. Phospholipids with C22:6 render membrane more flexible and facilitate membrane fission participating in the formation of vesicles [73, 74]. The BMP polyunsaturation coupled to its cone-shape structure is considered to be crucial for the dynamic of endolysosomal membranes and the formation of ILVs [18]. All these elements could explain the increase of BMP docosahexaenoyl species in urinary endosome-derived EVs of our study.

5. Conclusions

In summary, current knowledge on the unconventional lipid BMP outlines its crucial intracellular role to control the trafficking and degradation of proteins and lipids through the acidic endolysosomal compartment. Its accumulation in cells and tissues appeared as a cellular adaptation of the endosomal system to compensate for the increase of undigested material during various drug-induced and genetic LSDs such as Niemann Pick diseases, neuronal ceroid lipofuscinoses, mucopolysaccharidoses as well as recently with atherogenic-inducing diet [56, 75-78]. In addition, BMP release in biological fluids suggested its importance as a diagnostic biomarker of endolysosomal dysfunction during these diseases [28, 37, 56, 79]. Our present work confirmed this role for the first time in amiodarone-treated patient urines. Furthermore, the increased release of BMP-containing exosomes in urines could appear as an alternative to remove quickly excess of undigested material before irreversible toxicity as it was recently suggested for the clearance of toxic aggregates in neurodegenerative diseases [23]. Finally due to its ubiquitous distribution in most mammalian cells and its selective subcellular localization in the endolysosome, it can be speculated that BMP could be a specific lipid marker of endosome-derived EVs. However, this will require further analysis in EVs isolated from various extracellular biofluids. Thus, our present data could have implications not only in the field of all the disorders associated with endolysosomal dysfunction, but also in the growing field of EV research.

Funding: MR is supported by a PhD fellowship from the French Ministery of education. Financial supports were from INSERM; the University of Bern; SFD (Société Francophone du Diabète_AE 2016) and VML (Vaincre les Maladies Lysosomales_convention AO2018-6) to FHM.

Author contributions: MR performed most experiments; VL carried out lipid analysis of rat samples; FHM, AD and EEC performed microscopy analysis; AJ and PC helped for exosome purification; FHM and BF developed LC-MS/MS analysis; AV, PM and CB collected the patients samples; CS performed animal experiment; MdF performed biological analysis; RK and ADr helped for primary human macrophage isolation and confocal microscopy analysis; FHM designed the research project with contribution of ID, PM, CC and SR, and wrote the manuscript. All the authors discussed the data and agreed with the manuscript.

Acknowledgements: The authors thank all the clinical staff of the endocrinology-cardiology ward for help in collecting urines. The authors are also thankful to Dr Harout Iliozer for clinical information, to members of the Draeger laboratory for help and to Mr A. Debein for animal feeding.

Conflict of interest: the authors declared no competing financial interest.

References

[1] T. Kobayashi, M.H. Beuchat, M. Lindsay, S. Frias, R.D. Palmiter, H. Sakuraba, R.G. Parton, J. Gruenberg, Late endosomal membranes rich in lysobisphosphatidic acid regulate cholesterol transport, Nat Cell Biol, 1 (1999) 113-118.
[2] F. Hullin-Matsuda, C. Luquain-Costaz, J. Bouvier, I. Delton-Vandenbroucke, Bis(monoacylglycero)phosphate, a peculiar phospholipid to control the fate of cholesterol: Implications in pathology, Prostaglandins Leukot Essent Fatty Acids, 81 (2009) 313-324.
[3] H.D. Gallala, K. Sandhoff, Biological function of the cellular lipid BMP-BMP as a key activator for cholesterol sorting and membrane digestion, Neurochem Res, 36 (2011) 1594-1600.
[4] J. Gruenberg, Life in the lumen: The multivesicular endosome, Traffic, 21 (2020) 76-93.
[5] M. Waite, V. Roddick, T. Thornburg, L. King, F. Cochran, Conversion of phosphatidylglycerol to lyso(bis)phosphatidic acid by alveolar macrophages, Faseb J, 1 (1987) 318-325.
[6] F. Hullin-Matsuda, K. Kawasaki, I. Delton-Vandenbroucke, Y. Xu, M. Nishijima, M. Lagarde, M. Schlame, T. Kobayashi, De novo biosynthesis of the late endosome lipid, bis(monoacylglycero)phosphate, J Lipid Res, 48 (2007) 1997-2008.
[7] J. Bouvier, K.A. Zemski Berry, F. Hullin-Matsuda, A. Makino, S. Michaud, A. Geloen, R.C. Murphy, T. Kobayashi, M. Lagarde, I. Delton-Vandenbroucke, Selective decrease of bis(monoacylglycero)phosphate content in macrophages by high supplementation with docosahexaenoic acid, J Lipid Res, 50 (2009) 243-255.
[8] T. Kobayashi, M.H. Beuchat, J. Chevallier, A. Makino, N. Mayran, J.M. Escola, C. Lebrand, P. Cosson, J. Gruenberg, Separation and characterization of late endosomal membrane domains, J Biol Chem, 277 (2002) 32157-32164.
[9] H.H. Tan, A. Makino, K. Sudesh, P. Greimel, T. Kobayashi, Spectroscopic evidence for the unusual stereochemical configuration of an endosome-specific lipid, Angew Chem Int Ed Engl, 51 (2012) 533-535.
[10] B. Breiden, K. Sandhoff, Lysosomal Glycosphingolipid Storage Diseases, Annual review of biochemistry, 88 (2019) 461-485.
[11] T. Kobayashi, E. Stang, K.S. Fang, P. de Moerloose, R.G. Parton, J. Gruenberg, A lipid associated with the antiphospholipid syndrome regulates endosome structure and function, Nature, 392 (1998) 193-197.
[12] C.l. Luquain-Costaz, E. Lefai, M. Arnal-Levron, D. Markina, S. SakaÃ¯, V. Euthine, A. Makino, M. Guichardant, S. Yamashita, T. Kobayashi, M. Lagarde, P. Moulin, I. Delton-Vandenbroucke, Bis(Monoacylglycero)Phosphate Accumulation in Macrophages Induces Intracellular Cholesterol Redistribution, Attenuates Liver-X Receptor/ATP-Binding Cassette Transporter A1/ATP-Binding Cassette Transporter G1 Pathway, and Impairs Cholesterol Efflux, Arteriosclerosis, Thrombosis, and Vascular Biology, 33 (2013) 1803-1811.
[13] H. Schulze, T. Kolter, K. Sandhoff, Principles of lysosomal membrane degradation Cellular topology and biochemistry of lysosomal lipid degradation, Biochim Biophys Acta, 1793 (2009) 674-683.
[14] M. Arnal-Levron, Y. Chen, P. Greimel, F. Calevro, K. Gaget, F. Riols, A. Batut, J. Bertrand-Michel, F. Hullin-Matsuda, V.M. Olkkonen, I. Delton, C. Luquain-Costaz, Bis(monoacylglycero)phosphate regulates oxysterol binding protein-related protein 11 dependent sterol trafficking, Biochim Biophys Acta Mol Cell Biol Lipids, 1864 (2019) 1247-1257.
[15] K. Stadler, H.R. Ha, V. Ciminale, C. Spirli, G. Saletti, M. Schiavon, D. Bruttomesso, L. Bigler, F. Follath, A. Pettenazzo, A. Baritussio, Amiodarone alters late endosomes and inhibits SARS coronavirus infection at a post-endosomal level, American journal of respiratory cell and molecular biology, 39 (2008) 142-149.

[16] E. Zaitseva, S.-T. Yang, K. Melikov, S. Pourmal, L.V. Chernomordik, Dengue Virus Ensures Its Fusion in Late Endosomes Using Compartment-Specific Lipids, PLoS Pathog, 6 (2010) e1001131.
[17] C. Luquain, R. Dolmazon, J.M. Enderlin, C. Laugier, M. Lagarde, J.F. Pageaux, Bis(monoacylglycerol) phosphate in rat uterine stromal cells: structural characterization and specific esterification of docosahexaenoic acid, Biochem J, 351 Pt 3 (2000) 795-804.
[18] H. Matsuo, J. Chevallier, N. Mayran, I. Le Blanc, C. Ferguson, J. Faure, N.S. Blanc, S. Matile, J. Dubochet, R. Sadoul, R.G. Parton, F. Vilbois, J. Gruenberg, Role of LBPA and Alix in multivesicular liposome formation and endosome organization, Science, 303 (2004) 531-534.
[19] G. van Niel, G. D'Angelo, G. Raposo, Shedding light on the cell biology of extracellular vesicles, Nat Rev Mol Cell Biol, 19 (2018) 213-228.
[20] M. Record, K. Carayon, M. Poirot, S. Silvente-Poirot, Exosomes as new vesicular lipid transporters involved in cell-cell communication and various pathophysiologies, Biochimica et biophysica acta, 1841 (2014) 108-120.
[21] R. Wubbolts, R.S. Leckie, P.T. Veenhuizen, G. Schwarzmann, W. Mobius, J. Hoernschemeyer, J.W. Slot, H.J. Geuze, W. Stoorvogel, Proteomic and biochemical analyses of human B cell-derived exosomes. Potential implications for their function and multivesicular body formation, The Journal of biological chemistry, 278 (2003) 10963-10972.
[22] K. Laulagnier, C. Motta, S. Hamdi, S. Roy, F. Fauvelle, J.F. Pageaux, T. Kobayashi, J.P. Salles, B. Perret, C. Bonnerot, M. Record, Mast cell- and dendritic cell-derived exosomes display a specific lipid composition and an unusual membrane organization, Biochem J, 380 (2004) 161-171.
[23] A.M. Miranda, Z.M. Lasiecka, Y. Xu, J. Neufeld, S. Shahriar, S. Simoes, R.B. Chan, T.G. Oliveira, S.A. Small, G. Di Paolo, Neuronal lysosomal dysfunction releases exosomes harboring APP C-terminal fragments and unique lipid signatures, Nature communications, 9 (2018) 291.
[24] N.P. Hessvik, A. Llorente, Current knowledge on exosome biogenesis and release, Cellular and molecular life sciences : CMLS, 75 (2018) 193-208.
[25] M. Mathieu, L. Martin-Jaular, G. Lavieu, C. Thery, Specificities of secretion and uptake of exosomes and other extracellular vesicles for cell-to-cell communication, Nat Cell Biol, 21 (2019) 9-17.
[26] S. Rome, A. Forterre, M.L. Mizgier, K. Bouzakri, Skeletal Muscle-Released Extracellular Vesicles: State of the Art, Front Physiol, 10 (2019) 929.
[27] K.L. Thompson, J. Zhang, S. Stewart, B.A. Rosenzweig, K. Shea, D. Mans, T. Colatsky, Comparison of urinary and serum levels of di-22:6-bis(monoacylglycerol)phosphate as noninvasive biomarkers of phospholipidosis in rats, Toxicol Lett, 213 (2012) 285-291.
[28] P.J. Meikle, S. Duplock, D. Blacklock, P.D. Whitfield, G. Macintosh, J.J. Hopwood, M. Fuller, Effect of lysosomal storage on bis(monoacylglycero)phosphate, Biochem J, 411 (2008) 71-78.
[29] H. Sawada, K. Takami, S. Asahi, A toxicogenomic approach to drug-induced phospholipidosis: analysis of its induction mechanism and establishment of a novel in vitro screening system, Toxicol Sci, 83 (2005) 282-292.
[30] Anderson, Borlak, Drug-induced phospholipidosis, FEBS Letters, 580 (2006) 5533-5540.
[31] N. Bocchini, M. Giantin, F. Crivellente, S. Ferraresso, I. Faustinelli, M. Dacasto, P. Cristofori, Molecular biomarkers of phospholipidosis in rat blood and heart after amiodarone treatment, J Appl Toxicol, 35 (2015) 90-103.
[32] M.J. Reasor, A review of the biology and toxicologic implications of the induction of lysosomal lamellar bodies by drugs, Toxicology and applied pharmacology, 97 (1989) 47-56.
[33] K.L. Thompson, K. Haskins, B.A. Rosenzweig, S. Stewart, J. Zhang, D. Peters, A. Knapton, R. Rouse, D. Mans, T. Colatsky, Comparison of the diagnostic accuracy of di-22:6-bis(monoacylglycerol)phosphate and other urinary phospholipids for drug-induced phospholipidosis or tissue injury in the rat, Int J Toxicol, 31 (2012) 14-24.

[34] M. Wang, J.P. Palavicini, A. Cseresznye, X. Han, Strategy for Quantitative Analysis of Isomeric Bis(monoacylglycero)phosphate and Phosphatidylglycerol Species by Shotgun Lipidomics after One-Step Methylation, Analytical chemistry, 89 (2017) 8490-8495.
[35] M. Scherer, G. Schmitz, G. Liebisch, Simultaneous quantification of cardiolipin, bis(monoacylglycero)phosphate and their precursors by hydrophilic interaction LC-MS/MS including correction of isotopic overlap, Analytical chemistry, 82 (2010) 8794-8799.
[36] E.A. Tengstrand, G.T. Miwa, F.Y. Hsieh, Bis(monoacylglycerol)phosphate as a non-invasive biomarker to monitor the onset and time-course of phospholipidosis with drug-induced toxicities, Expert Opin Drug Metab Toxicol, 6 (2010) 555-570.
[37] N. Liu, E.A. Tengstrand, L. Chourb, F.Y. Hsieh, Di-22:6-bis(monoacylglycerol)phosphate: A clinical biomarker of drug-induced phospholipidosis for drug development and safety assessment, Toxicology and Applied Pharmacology, 279 (2014) 467-476.
[38] S. Basaria, D.S. Cooper, Amiodarone and the thyroid, Am J Med, 118 (2005) 706-714.
[39] P. Zimetbaum, Amiodarone for atrial fibrillation, The New England journal of medicine, 356 (2007) 935-941.
[40] W. Tsang, R.L. Houlden, Amiodarone-induced thyrotoxicosis: a review, Can J Cardiol, 25 (2009) 421-424.
[41] P. Vassallo, R.G. Trohman, Prescribing amiodarone: an evidence-based review of clinical indications, JAMA, 298 (2007) 1312-1322.
[42] N. Mesens, M. Desmidt, G.R. Verheyen, S. Starckx, S. Damsch, R. De Vries, M. Verhemeldonck, J. Van Gompel, A. Lampo, L. Lammens, Phospholipidosis in rats treated with amiodarone: serum biochemistry and whole genome micro-array analysis supporting the lipid traffic jam hypothesis and the subsequent rise of the biomarker BMP, Toxicol Pathol, 40 (2012) 491-503.
[43] Y. Chen, M. Arnal-Levron, M. Lagarde, P. Moulin, C. Luquain-Costaz, I. Delton, THP1 macrophages oxidized cholesterol, generating 7-derivative oxysterols specifically released by HDL, Steroids, 99 (2015) 212-218.
[44] Y. Larpin, H. Besancon, M.I. Iacovache, V.S. Babiychuk, E.B. Babiychuk, B. Zuber, A. Draeger, R. Koffel, Bacterial pore-forming toxin pneumolysin: Cell membrane structure and microvesicle shedding capacity determines differential survival of cell types, FASEB J, 34 (2020) 1665-1678.
[45] R. Koffel, A. Meshcheryakova, J. Warszawska, A. Hennig, K. Wagner, A. Jorgl, D. Gubi, D. Moser, A. Hladik, U. Hoffmann, M.B. Fischer, W. van den Berg, M. Koenders, C. Scheinecker, B. Gesslbauer, S. Knapp, H. Strobl, Monocytic cell differentiation from band-stage neutrophils under inflammatory conditions via MKK6 activation, Blood, 124 (2014) 2713-2724.
[46] E.G. Bligh, W.J. Dyer, A rapid method of total lipid extraction and purification, Can J Biochem Physiol, 37 (1959) 911-917.
[47] A.H. Gheinani, M. Vogeli, U. Baumgartner, E. Vassella, A. Draeger, F.C. Burkhard, K. Monastyrskaya, Improved isolation strategies to increase the yield and purity of human urinary exosomes for biomarker discovery, Sci Rep, 8 (2018) 3945.
[48] P. Fernandez-Llama, S. Khositseth, P.A. Gonzales, R.A. Star, T. Pisitkun, M.A. Knepper, Tamm-Horsfall protein and urinary exosome isolation, Kidney international, 77 (2010) 736-742.
[49] A. Forterre, A. Jalabert, E. Berger, M. Baudet, K. Chikh, E. Errazuriz, J. De Larichaudy, S. Chanon, M. Weiss-Gayet, A.M. Hesse, M. Record, A. Geloen, E. Lefai, H. Vidal, Y. Coute, S. Rome, Proteomic analysis of C2C12 myoblast and myotube exosome-like vesicles: a new paradigm for myoblast-myotube cross talk?, PloS one, 9 (2014) e84153.
[50] A. Forterre, A. Jalabert, K. Chikh, S. Pesenti, V. Euthine, A. Granjon, E. Errazuriz, E. Lefai, H. Vidal, S. Rome, Myotube-derived exosomal miRNAs downregulate Sirtuin1 in myoblasts during muscle cell differentiation, Cell cycle, 13 (2014) 78-89.

[51] E.T. Baronas, J.W. Lee, C. Alden, F.Y. Hsieh, Biomarkers to monitor drug-induced phospholipidosis, Toxicol Appl Pharmacol, 218 (2007) 72-78.
[52] J.R. Wherrett, S. Huterer, Bis-(monoacylglyceryl)-phosphate of rat and human liver: fatty acid composition and NMR spectroscopy, Lipids, 8 (1973) 531-533.
[53] Q. Chen, R. Takada, C. Noda, S. Kobayashi, S. Takada, Different populations of Wnt-containing vesicles are individually released from polarized epithelial cells, Sci Rep, 6 (2016) 35562.
[54] J. Wang, Y. Yao, J. Wu, G. Li, Identification and analysis of exosomes secreted from macrophages extracted by different methods, Int J Clin Exp Pathol, 8 (2015) 6135-6142.
[55] K. Kumar, P.J. Zimetbaum, Antiarrhythmic drugs 2013: state of the art, Curr Cardiol Rep, 15 (2013) 410.
[56] G.F. Grabner, N. Fawzy, M.A. Pribasnig, M. Trieb, U. Taschler, M. Holzer, M. Schweiger, H. Wolinski, D. Kolb, A. Horvath, R. Breinbauer, T. Rülicke, R. Rabl, A. Lass, V. Stadlbauer, B. Hutter-Paier, R.E. Stauber, P. Fickert, R. Zechner, G. Marsche, T.O. Eichmann, R. Zimmermann, Metabolic disease and ABHD6 alter the circulating bis(monoacylglycerol)phosphate profile in mice and humans, Journal of Lipid Research, 60 (2019) 1020-1031.
[57] J. Massart, K. Begriche, C. Moreau, B. Fromenty, Role of nonalcoholic fatty liver disease as risk factor for drug-induced hepatotoxicity, J Clin Transl Res, 3 (2017) 212-232.
[58] G. Morissette, A. Ammoury, D. Rusu, M.C. Marguery, R. Lodge, P.E. Poubelle, F. Marceau, Intracellular sequestration of amiodarone: role of vacuolar ATPase and macroautophagic transition of the resulting vacuolar cytopathology, British journal of pharmacology, 157 (2009) 1531-1540.
[59] E. Piccoli, M. Nadai, C.M. Caretta, V. Bergonzini, C. Del Vecchio, H.R. Ha, L. Bigler, D. Dal Zoppo, E. Faggin, A. Pettenazzo, R. Orlando, C. Salata, A. Calistri, G. Palu, A. Baritussio, Amiodarone impairs trafficking through late endosomes inducing a Niemann-Pick C-like phenotype, Biochemical pharmacology, 82 (2011) 1234-1249.
[60] W.H. Fissell, J.H. Miner, What Is the Glomerular Ultrafiltration Barrier?, Journal of the American Society of Nephrology : JASN, 29 (2018) 2262-2264.
[61] F.J. Verweij, C. Revenu, G. Arras, F. Dingli, D. Loew, D.M. Pegtel, G. Follain, G. Allio, J.G. Goetz, P. Zimmermann, P. Herbomel, F. Del Bene, G. Raposo, G. van Niel, Live Tracking of Inter-organ Communication by Endogenous Exosomes In Vivo, Dev Cell, 48 (2019) 573-589 e574.
[62] D.K. Jeppesen, A.M. Fenix, J.L. Franklin, J.N. Higginbotham, Q. Zhang, L.J. Zimmerman, D.C. Liebler, J. Ping, Q. Liu, R. Evans, W.H. Fissell, J.G. Patton, L.H. Rome, D.T. Burnette, R.J. Coffey, Reassessment of Exosome Composition, Cell, 177 (2019) 428-445 e418.
[63] J.W. Dear, J.M. Street, M.A. Bailey, Urinary exosomes: a reservoir for biomarker discovery and potential mediators of intrarenal signalling, Proteomics, 13 (2013) 1572-1580.
[64] M.L. Merchant, I.M. Rood, J.K.J. Deegens, J.B. Klein, Isolation and characterization of urinary extracellular vesicles: implications for biomarker discovery, Nat Rev Nephrol, 13 (2017) 731-749.
[65] L. Wang, T. Skotland, V. Berge, K. Sandvig, A. Llorente, Exosomal proteins as prostate cancer biomarkers in urine: From mass spectrometry discovery to immunoassay-based validation, Eur J Pharm Sci, 98 (2017) 80-85.
[66] A.L. Stahl, K. Johansson, M. Mossberg, R. Kahn, D. Karpman, Exosomes and microvesicles in normal physiology, pathophysiology, and renal diseases, Pediatr Nephrol, 34 (2019) 11-30.
[67] T. Pisitkun, R.F. Shen, M.A. Knepper, Identification and proteomic profiling of exosomes in human urine, Proceedings of the National Academy of Sciences of the United States of America, 101 (2004) 13368-13373.
[68] C. Thery, K.W. Witwer *et al*, Minimal information for studies of extracellular vesicles 2018 (MISEV2018): a position statement of the International Society for Extracellular Vesicles and update of the MISEV2014 guidelines, J Extracell Vesicles, 7 (2018) 1535750.

[69] T. Skotland, K. Sandvig, A. Llorente, Lipids in exosomes: Current knowledge and the way forward, Prog Lipid Res, 66 (2017) 30-41.
[70] M. Record, S. Silvente-Poirot, M. Poirot, M.J.O. Wakelam, Extracellular vesicles: lipids as key components of their biogenesis and functions, Journal of lipid research, 59 (2018) 1316-1324.
[71] C. Bissig, M. Lenoir, M.C. Velluz, I. Kufareva, R. Abagyan, M. Overduin, J. Gruenberg, Viral infection controlled by a calcium-dependent lipid-binding module in ALIX, Dev Cell, 25 (2013) 364-373.
[72] W. Mobius, E. van Donselaar, Y. Ohno-Iwashita, Y. Shimada, H.F. Heijnen, J.W. Slot, H.J. Geuze, Recycling compartments and the internal vesicles of multivesicular bodies harbor most of the cholesterol found in the endocytic pathway, Traffic, 4 (2003) 222-231.
[73] M. Pinot, S. Vanni, S. Pagnotta, S. Lacas-Gervais, L.-A. Payet, T. Ferreira, R. Gautier, B. Goud, B. Antonny, H. Barelli, Polyunsaturated phospholipids facilitate membrane deformation and fission by endocytic proteins, Science, 345 (2014) 693-697.
[74] M.M. Manni, M.L. Tiberti, S. Pagnotta, H. Barelli, R. Gautier, B. Antonny, Acyl chain asymmetry and polyunsaturation of brain phospholipids facilitate membrane vesiculation without leakage, Elife, 7 (2018).
[75] M.T. Vanier, Complex lipid trafficking in Niemann-Pick disease type C, Journal of inherited metabolic disease, 38 (2015) 187-199.
[76] Z. Akgoc, M. Sena-Esteves, D.R. Martin, X. Han, A. d'Azzo, T.N. Seyfried, Bis(monoacylglycero)phosphate: a secondary storage lipid in the gangliosidoses, Journal of lipid research, 56 (2015) 1006-1013.
[77] K. Kitakaze, Y. Mizutani, E. Sugiyama, C. Tasaki, D. Tsuji, N. Maita, T. Hirokawa, D. Asanuma, M. Kamiya, K. Sato, M. Setou, Y. Urano, T. Togawa, A. Otaka, H. Sakuraba, K. Itoh, Protease-resistant modified human beta-hexosaminidase B ameliorates symptoms in GM2 gangliosidosis model, The Journal of clinical investigation, 126 (2016) 1691-1703.
[78] F.M. Platt, Emptying the stores: lysosomal diseases and therapeutic strategies, Nat Rev Drug Discov, 17 (2018) 133-150.
[79] M.T. Vanier, P. Gissen, P. Bauer, M.J. Coll, A. Burlina, C.J. Hendriksz, P. Latour, C. Goizet, R.W. Welford, T. Marquardt, S.A. Kolb, Diagnostic tests for Niemann-Pick disease type C (NP-C): A critical review, Molecular genetics and metabolism, 118 (2016) 244-254.

Figure legends

Figure 1: **Amiodarone increases diC22:6-BMP in rat urine and modifies its renal clearance.** Male Wistar rats were treated or not with amiodarone (A50 and A150, 50 and 150 mg/kg/day, respectively) and lipid extracts of liver, urine and plasma were analyzed by LC-MS/MS. **A) the effect of amiodarone on liver** was evaluated by diC22:6-BMP liver content (expressed in pmol/mg proteins); levels of hepatic transaminases AST, ALT in plasma (expressed in UI/L) and liver weight (expressed in percentage of body weight); **B) diC22:6-BMP content** was analyzed in urine and plasma and is expressed in pmol corrected to µmol of creatinine for urine and in pmol/ ml of plasma; **C) the effect of amiodarone on kidney** was evaluated by the content of creatinine and proteins in the 24hr-urine. The renal clearance of creatinine and diC22:6-BMP was calculated as described in Material and Methods and is expressed in ml/min. All values are mean ± sem of n=3 for control (white bars) and amiodarone-treated (A50, grey bars; A150, black bars) rats. * $p<0.05$ of unpaired Student's t test compared to control.

Figure 2: Amiodarone increases BMP content in human urine. Lipid extracts of urine from control subjects, amiodarone-treated patients and NASH patients were analyzed by LC-MS/MS. diC22:6-BMP species (**A**) and total BMP (**B**) content is expressed in pmol corrected to µmol of creatinine and is mean ± sem of n=12, control subjects (white bars); n=24, amiodarone-treated patients (black bars) and n=6, NASH patients (without amiodarone treatment; grey bars). * $p<0.05$ of unpaired Student's t test compared to control subjects and to NASH patients. **C**) Schematic representation of unsaturation degree of BMP molecular species with significant increase of polyunsaturated species after amiodarone treatment content. Saturated species correspond to species with fatty acid without double bond, monounsaturated species to species with fatty acid containing one double bond and polyunsaturated to species with fatty acid containing 2 or more double bonds. Values are expressed as mole% and are mean of the data presented in Table 2. * $p<0.05$ of unpaired Student's t test compared to control subjects.

Figure 3: **Amiodarone increases the secretion of BMP-containing extracellular vesicles into human urine.** Extracellular vesicles (EVs) were purified from 50ml urines of control subjects (n=3) and amiodarone-treated patients (n=3) as described in Material and Methods and recovered by 100 µl PBS. **A)** The total protein content (quantified by Bradford assay) of EVs and diC22:6-BMP content (analyzed by LC-MS/MS) in the 200 x g-urine supernatant and urinary EVs from amiodarone-treated patients (black bars) are expressed in fold increase of the control subjects (white bars) (mean ± sem, n=3). * $p<0.05$ of unpaired Student's t test compared to control subjects. **B)** Equal volume of each purified EV corresponding to 2 to 5 µg of EV proteins was analyzed by Western blot with antibodies against classical EV protein markers ALIX, CD63 and TSG101: EVs from three control subjects (lane

2 to 4) and three amiodarone-treated patients (lane 5 to 7). Human embryonic kidney HEK293 cell extract (lane 1) corresponding to 24 µg proteins was used as positive standard.

Figure 4: **BMP co-localizes with exosome protein marker CD63 in EVs isolated from human urine**: EVs purified from urine of control subject were analyzed by immunogold electron microscopy with primary antibodies against the exosome protein marker CD63 (**A**, both panels) or the endolysosomal lipid BMP (**B**, both panels), then with 10nm gold-conjugated secondary antibodies. Immuno-double labeling (**C**, both panels) was performed with CD63 (5nm-conjugated secondary antibody) and BMP (15nm gold-conjugated secondary antibody). Scale bar, 100 nm (red values indicate the vesicle diameter in nm).

Figure 5: **BMP co-localizes with exosome protein marker CD63 in EVs isolated from conditioned medium of HEK293 cells**: EVs purified from the conditioned medium of human embryonic kidney HEK293 cells were labeled with primary antibodies against the exosome protein marker CD63 (upper panel) or with BMP (middle panel), then with 10nm gold-conjugated secondary antibodies. Co-labeling (lower panel) was performed with CD63 (5nm-conjugated secondary antibody) and BMP (15nm gold-conjugated secondary antibody). Scale bar, 100 nm (red values indicate the vesicle diameter in nm).

Figure 6: **Amiodarone modifies the acidic endolysosomal compartment of human macrophages.** Primary human monocytes (**A**) and human THP-1 cells (**B**) differentiated into macrophages were non-treated (=control) or treated with 10µM of amiodarone (=Amio) for 24hr. At the end of the treatment, they were incubated with LysoTracker DND99 (red) to label the acidic organelles. After fixation, they were successively incubated with the primary antibody against the late endosomal lipid, BMP and A488-conjugated secondary antibody (green). Slides were analyzed by fluorescent confocal microscopy. Bar = 10µm.

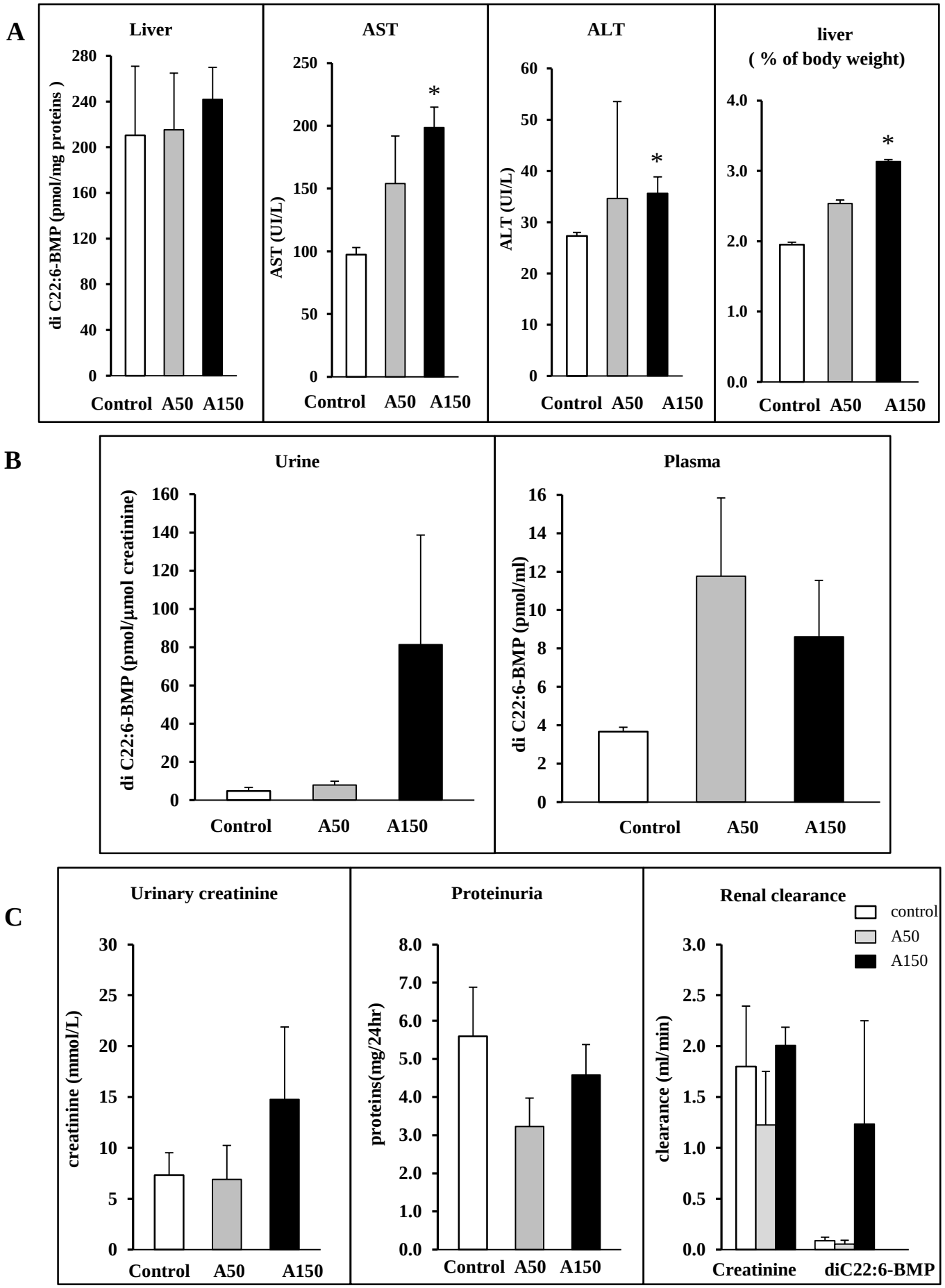
A
Liver
di C22:6-BMP (pmol/mg proteins)
280
240
200
160
120
80
40
0
Control A50 A150
AST
AST (UI/L)
250
200
150
100
50
0
*
Control A50 A150
ALT
ALT (UI/L)
60
50
40
30
20
10
0
*
Control A50 A150
liver
(% of body weight)
4.0
3.0
2.0
1.0
0.0
*
Control A50 A150
B
Urine
di C22:6-BMP (pmol/µmol creatinine)
160
140
120
100
80
60
40
20
0
Control A50 A150
Plasma
di C22:6-BMP (pmol/ml)
16
14
12
10
8
6
4
2
0
Control A50 A150
C
Urinary creatinine
creatinine (mmol/L)
30
25
20
15
10
5
0
Control A50 A150
Proteinuria
proteins(mg/24hr)
8.0
7.0
6.0
5.0
4.0
3.0
2.0
1.0
0.0
Control A50 A150
Renal clearance
control
A50
A150
clearance (ml/min)
3.0
2.5
2.0
1.5
1.0
0.5
0.0
Creatinine diC22:6-BMP

A

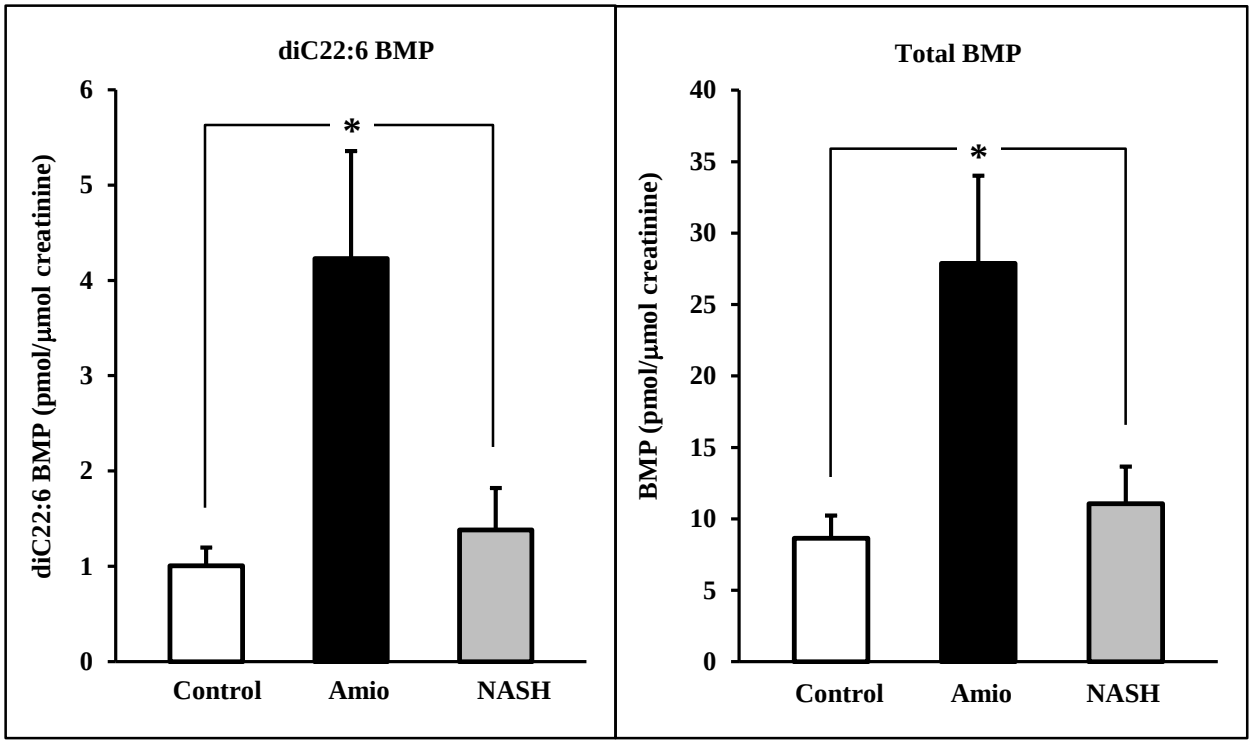
diC22:6 BMP
diC22:6 BMP (pmol/µmol creatinine)
6
5
4
3
2
1
0
*
Control
Amio
NASH
Total BMP
BMP (pmol/µmol creatinine)
40
35
30
25
20
15
10
5
0
*
Control
Amio
NASH

B

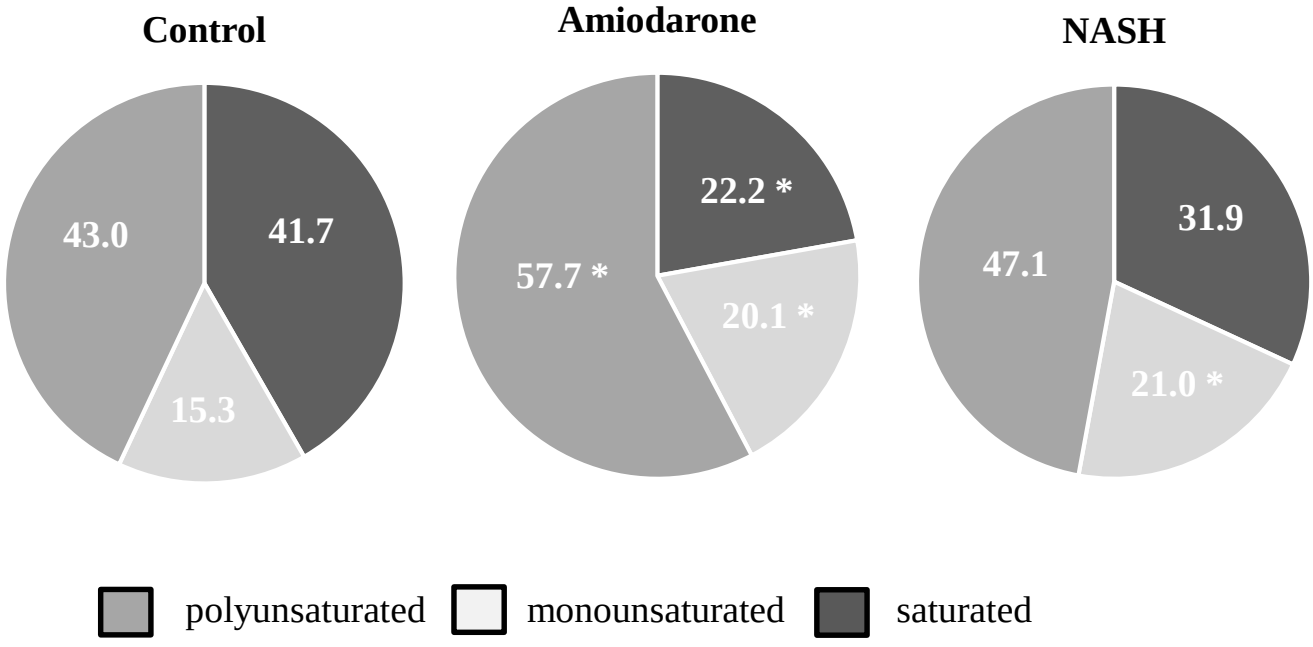
Control
43.0
41.7
15.3
Amiodarone
22.2 *
57.7 *
20.1 *
NASH
31.9
47.1
21.0 *
polyunsaturated
monounsaturated
saturated

Figure 3

A

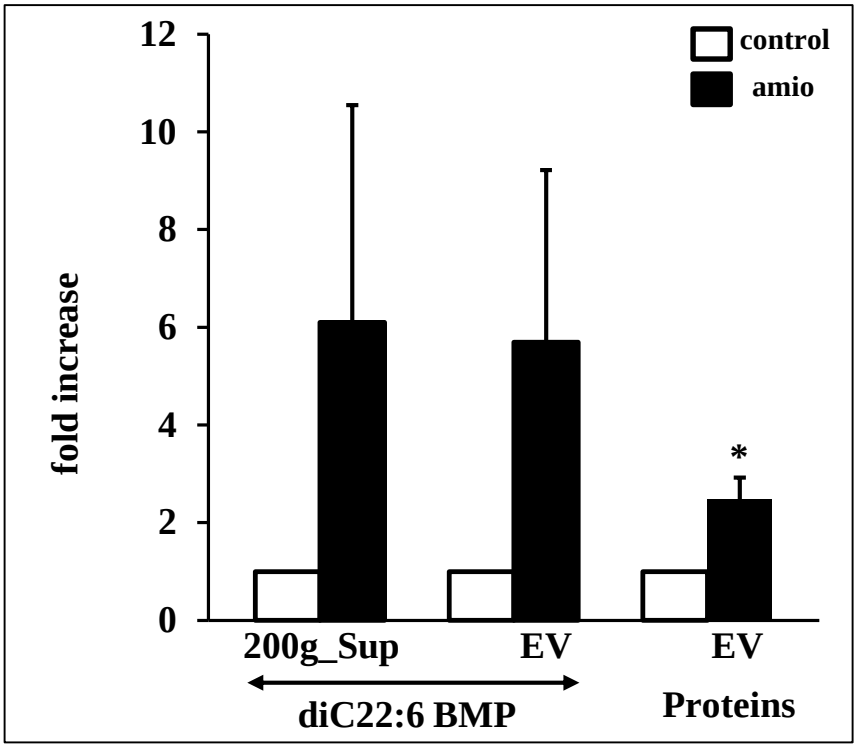
12
10
8
6
4
2
0
fold increase
control
amio
*
200g_Sup
EV
EV
Proteins
diC22:6 BMP

B

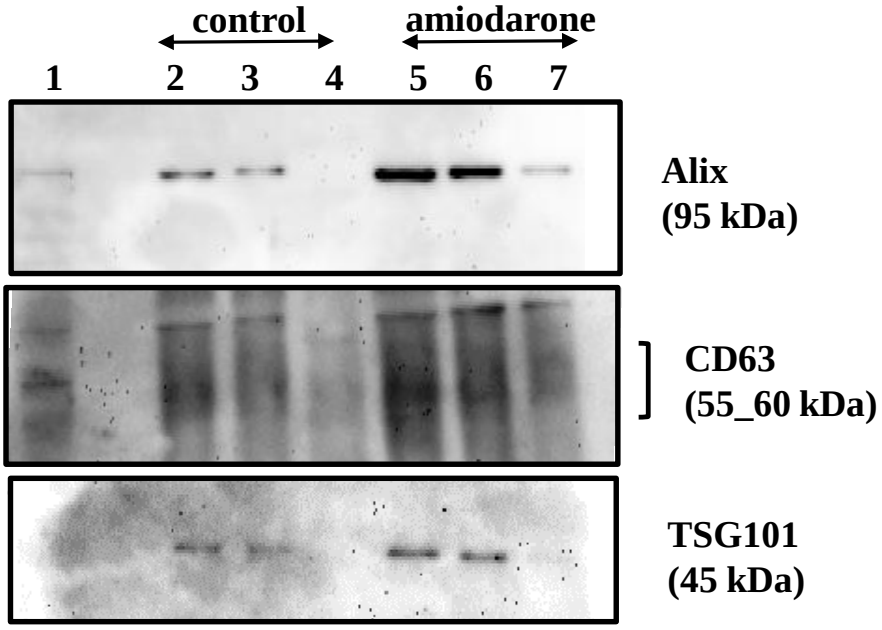
control
amiodarone
1
2
3
4
5
6
7
Alix
(95 kDa)
CD63
(55_60 kDa)
TSG101
(45 kDa)

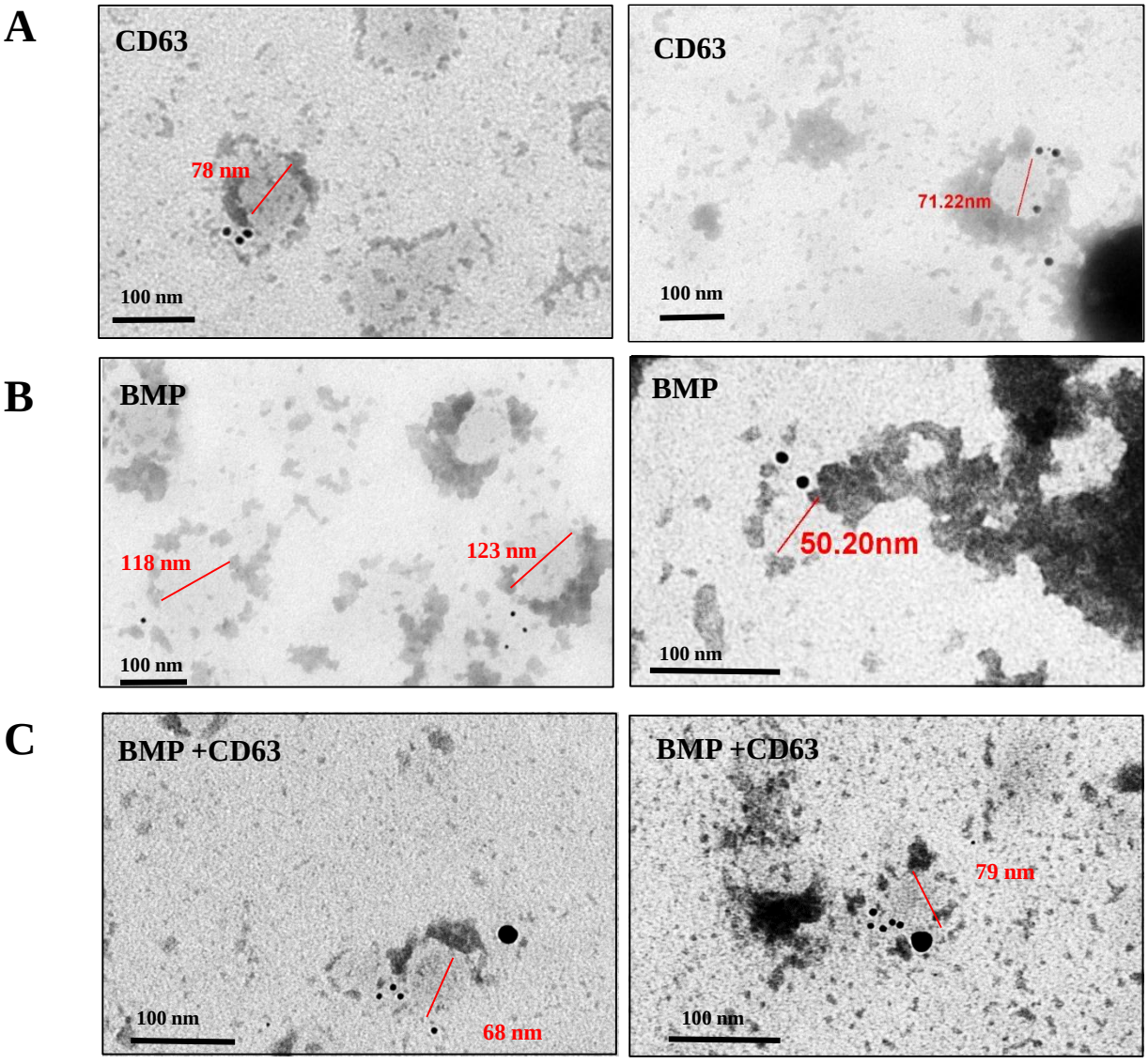
A
CD63
78 nm
100 nm
CD63
71.22nm
100 nm
B
BMP
118 nm
123 nm
100 nm
BMP
50.20nm
100 nm
C
BMP +CD63
100 nm
68 nm
BMP +CD63
79 nm
100 nm

Figure 5

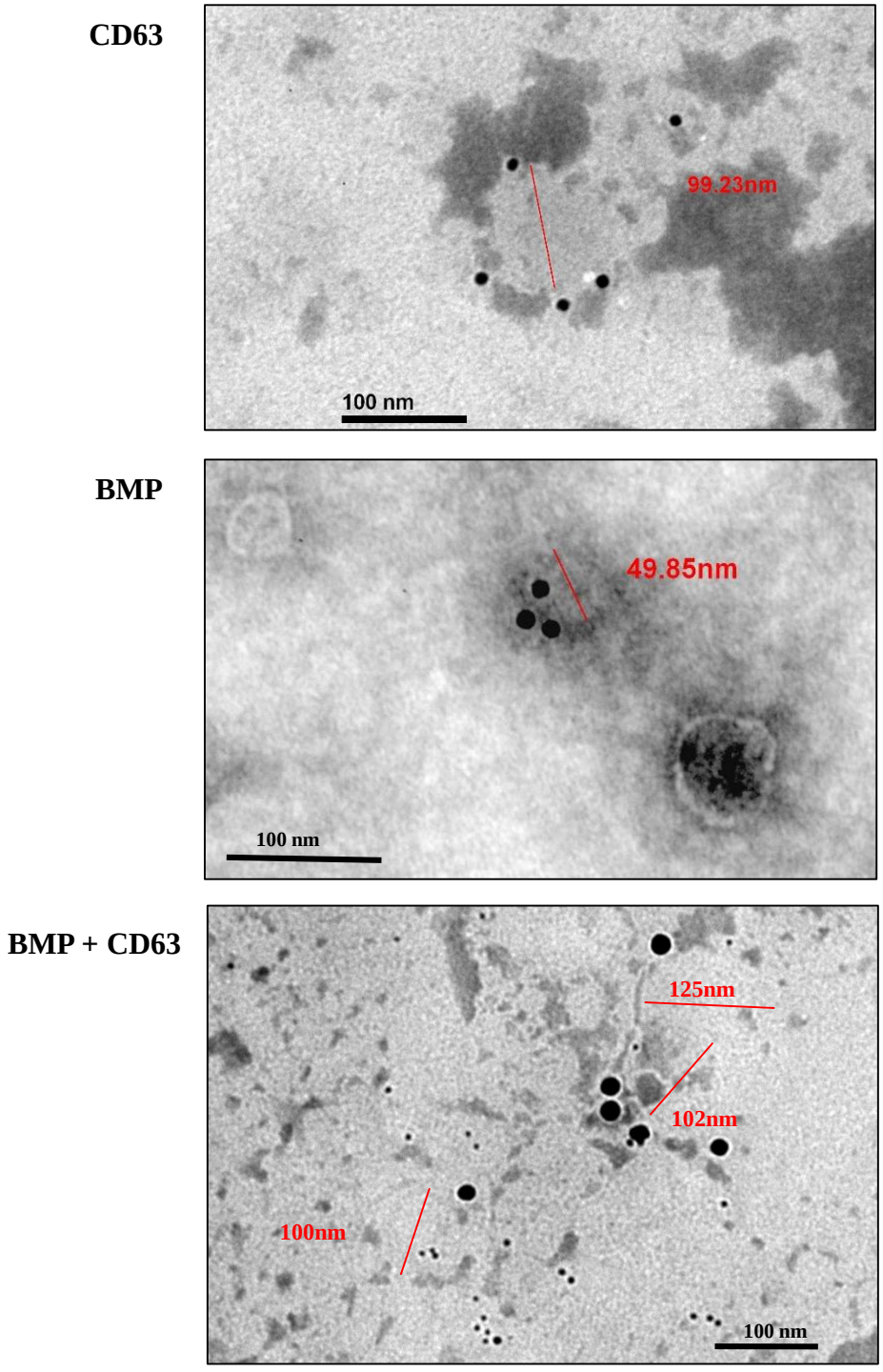
CD63
99.23nm
100 nm
BMP
49.85nm
100 nm
BMP + CD63
125nm
102nm
100nm
100 nm

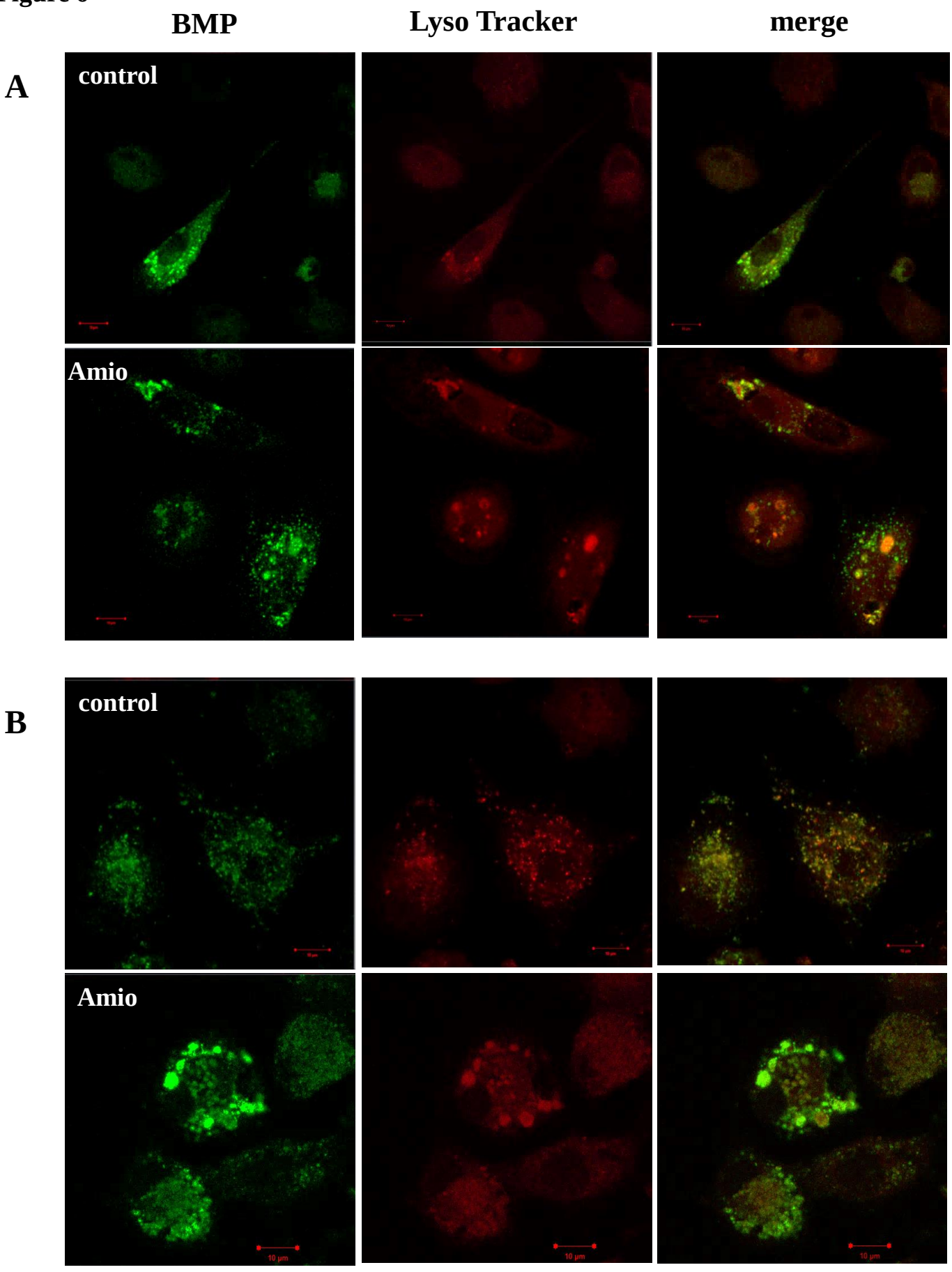
BMP
Lyso Tracker
merge
A
control
Amio
B
control
Amio
10 µm
10 µm
10 µm

Table 1: Characteritics of the human subjects

	Control subjects	Amiodarone patients	NASH patients
number (n)	12	24	6
age (years)	61 ± 2	71 ± 2	61 ± 7
women/men (n)	6/6	10/14	3/3
Amiodarone: average treatment length (months) ; oral daily dose (mg)	no	5_ 12; 200mg	no
Cardiomyopathy (n)	no	15	no
dysthyroidism (n)	no	6	no
hypothyroidism (n)	-	4	-
hyperthyroidism (n)	-	2	-
Biological parameters			
urinary creatinine (mmol/L)	9.2 ± 1.9	7.4 ± 0.8	9.3 ± 1.9
BMI (kg/m^2)	n.d	27 ± 1 [a]	39 ± 3
plasma AST (UI/L)	n.d	40 ± 13 [c]	36 ± 7
plasma ALT (UI/L)	n.d	50 ± 23 [d]	43 ± 11
plasma HbA1c (%)	n.d	6.9 ± 0.3 [d]	7.6 ± 0.4
plasma HDL cholesterol (g/L)	n.d	0.45 ±0.04 [c]	0.34 ± 0.05
plasma LDL cholesterol (g/L)	n.d	0.97 ±0.09 [b]	1.0 ± 0.2

Values are mean ± sem for n=12, control subjects; n=6, NASH patients; n=24, amiodarone-treated patients except [a], n=22; [b], n=20; [c], n=19 and [d], n=17. n.d, not determined. AST aspartate aminotransferase; ALT, alanine aminotransferase; BMI, body mass index; HbA1c, glycated hemoglobin.

Table 2: Variation of BMP molecular species in urine of control, amiodarone-treated and NASH patients.

BMP molecular species (pmol / µmol creatinine)	Control (n=12)	Amiodarone (n=24)	NASH (n=6)
C16:0,C16:0	3.40 ± 0.49	3.89 ± 0.68	3.24 ± 0.62
C18:1n-9,C20:1n-9	0.06 ± 0.01	0.24 ± 0.06 *	0.14 ± 0.04 *
C16:0,C18:1n-9	0.08 ± 0.01	0.34 ± 0.09 *	0.14 ± 0.05
C18:1n-9,C18:1n-9	0.99 ± 0.19	4.49 ± 1.18 *	1.57 ± 0.51
C18:0,C18:1n-9	0.27 ± 0.05	0.90 ± 0.21 *	0.49 ± 0.07 *
C16:0,C18:2n-6	0.02 ± 0.004	0.13 ± 0.04 *	0.04 ± 0.01
C18:2n-6,C18:2n-6	0.08 ± 0.02	0.66 ± 0.22 *	0.10 ± 0.03
C18:1n-9,C18:2n-6	0.54 ± 0.11	3.17 ± 0.95 *	0.75 ± 0.28
C18:0,C18:2n-6	0.05 ± 0.01	0.20 ± 0.06 *	0.06 ± 0.01
C18:2n-6,C22:6n-3	0.36 ± 0.06	1.90 ± 0.48 *	0.44 ± 0.12
C18:1n-9,C22:6n-3	1.05 ± 0.16	4.66 ± 1.13 *	1.66 ± 0.50
C18:0,C22:6n-3	0.10 ± 0.02	0.31 ± 0.07 *	0.17 ± 0.04
C16:0,C20:4n-6	0.03 ± 0.01	0.14 ± 0.03 *	0.05 ± 0.01
C20:4n-6,C22:6n-3	0.07 ± 0.01	0.43 ± 0.10 *	0.09 ± 0.02
C22:6n-3,C22:6n-3	1.01 ± 0.14	4.23 ± 1.13 *	1.38 ± 0.44
C16:0,C22:6n-3	0.38 ± 0.07	1.28 ± 0.34 *	0.50 ± 0.15
C18:1n-9,C20:4n-6	0.06 ± 0.01	0.36 ± 0.10 *	0.07 ± 0.02
C16:0,C22:5n-3/6	0.01 ± 0.004	0.05 ± 0.01 *	0.03 ± 0.01
C18:1n-9,C20:3n-6/9	0.06 ± 0.02	0.35 ± 0.10 *	0.09 ± 0.03
C18:1n-9,C20:2n-6	0.03 ± 0.01	0.15 ± 0.04 *	0.05 ± 0.02
BMP TOTAL	8.64 ± 1.12	27.88 ± 6.13 *	11.05 ± 2.60
saturated (species mole%)	41.7 ± 4.1	22.2 ± 3.0	31.9 ± 5.0
monounsaturated(species mole%)	15.3 ± 1.1	20.1 ± 1.4 *	21.0 ± 1.9 *
polyunsaturated (species mole%)	43.0 ± 3.4	57.1 ± 3.1 *	47.1 ± 3.8

Data analyzed by LC-MS/MS are expressed in pmol/ µmol creatinine and are mean ± sem . *indicates significant difference with the control subjects by Student's t test $p<0.05$.

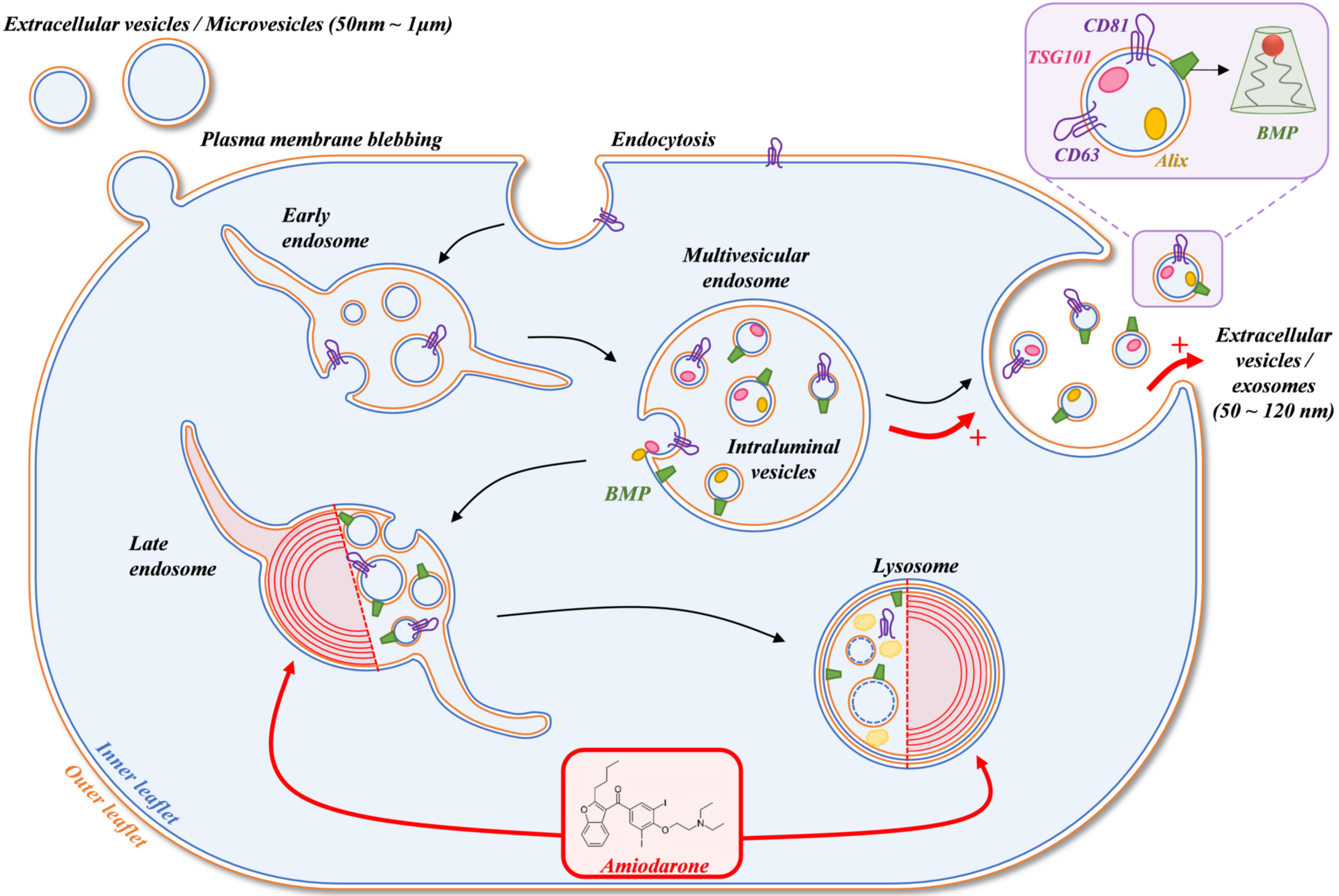

Drug-induced endolysosome dysfunction favors release of exosomes containing the cone-shape endosomal lipid BMP